Frontiers of Physics
https://doi.org/10.1007/s11467-021-1052-2
Front. Phys.
16(4), 43301 (2021)

REVIEW ARTICLE

Optoelectronic characteristics and application of black phosphorus and its analogs

Ying-Ying Li, Bo Gao†, Ying Han, Bing-Kun Chen, Jia-Yu Huo

College of Communication Engineering, Jilin University, Changchun 130012, China
Corresponding author. E-mail: †gaobo0312@jlu.edu.cn
Received November 19, 2020; accepted January 21, 2021

The tunable bandgap from 0.3 eV to 2 eV of black phosphorus (BP) makes it to fill the gap in graphene. When studying the properties of BP more comprehensive, scientists have discovered that many two-dimensional materials, such as tellurene, antimonene, bismuthene, indium selenide and tin sulfide, have similar structures and properties to black phosphorus thus called black phosphorus analogs. In this review, we briefly introduce preparation methods of black phosphorus and its analogs, with emphasis on the method of mechanical exfoliation (ME), liquid phase exfoliation (LPE) and chemical vapor deposition (CVD). And their characterization and properties according to their classification of single-element materials and multi-element materials are described. We focus on the performance of passively mode-locked fiber lasers using BP and its analogs as saturable absorbers (SA) and demonstrated this part through classification of working wavelength. Finally, we introduce the application of BP and its analogs, and discuss their future research prospects.

Keywords black phosphorus and its analogs, passively mode-locked fiber lasers, optoelectronic characteristics, saturable absorber

Contents

1 Introduction

In recent years, two-dimensional layered materials (2DLMs) represented by graphene have attracted wide attentions from scientists all over the world [1–6]. However, even though graphene has many excellent properties, its zero-bandgap properties largely hinder its applications such as in semiconductors as logic switches [7, 8]. The appearance of black phosphorus makes up for this deficiency [9–11]. Black phosphorus has excellent optoelectronic and nonlinear optical properties similar to graphene, as well as a tunable bandgap from 0.3 eV to 2 eV depending on the number of layers [12, 13], which allows it to have quite large modulation depth and very flexible working range.

In 1914, Bridgman reported a novel method to fabricate

*arXiv: 2102.13316. Special Topic: Black Phosphorus and Its Analogues (Eds. Xianhui Chen, Haibo Zeng, Han Zhang & Yuanbo Zhang). This article can also be found at http://journal.hep.com.cn/fop/EN/10.1007/s11467-021-1052-2.

black phosphorus at a moderate temperature (200 °C) and a high pressure (1.2 GPa) [14]. Since then, the research on BP has not made substantial progress. Until 2014, two groups of scientists, one from the United States and the other from China, successfully exfoliated black phosphorus down to two or three atomic layers [15]. After that, the study of the preparation, properties and applications of two-dimensional (2D) black phosphorus has become a hot topic [15–21]. While the mystery about the properties of black phosphorus was gradually revealed by scientists, they found that some materials have similar molecular structure and optoelectronic properties with black phosphorus [9, 22–24]. They simply named these materials as the black phosphorus analogs (i.e. tellurene, antimonene, bismuthene, indium selenide and tin sulfide) [25, 26].

With the rapid development of the laser field, scientists have recently paid more attention to the nonlinear optical properties of black phosphorus and its analogs, which allow them to be used in passively mode-locked fiber lasers as saturable absorbers to generate shorter pulses [27–32]. The basic thought of using saturable absorbers for pulse mode-locking is that when the light pulse passes through the absorber, the loss of the edge part is greater than the loss of the central part (which is strong enough to saturate the absorber), the light pulse is thus narrowed [33, 34]. According to above reasons, the parameters of saturable absorber play an important role in the generation of ultrashort pulses. Scientists noticed that black phosphorus and its analogs have outstanding and unique optical properties such as low saturation intensity, fast carrier mobility and so on [35–38]. To be more specific, large modulation depth and fast inter-band relaxation time are helpful to obtain narrower pulse in mode-locking fiber lasers. The low non-saturable absorption loss can effectively reduce the loss in the cavity and is more conducive to the formation of the pulse in the cavity. Meanwhile, black phosphorus and its analogs generally have the advantage of being small in size, which makes them easy to make into various forms of saturable absorbers to meet diverse needs.

Scientists have established models based on the electronic transition theory and two-stage band theory to better understand the nonlinear saturation absorption phenomenon of real saturable absorbers. This model is usually used to fit the data when calculating the parameters of saturable absorbers. The function of transmittance and incident light intensity is shown as follows:

$$\alpha(I) = \alpha_{\mathrm{s}}/(1 + I/I_{\mathrm{sat}}) + \alpha_{\mathrm{ns}},$$

where $\alpha(I)$ is absorption coefficient, α_{s} presents modulation depth, I_{sat} is the saturation intensity and α_{ns} is the non-saturable absorption loss. As shown in Fig. 1, Arof *et al.* [39] measured the nonlinear absorption curve of the saturable absorber based on BP using absorption technique. From the fitting curve, we can clearly observe that the modulation depth, saturation intensity and non-saturable absorption are 7.5%, 0.35 MW/cm^2, 57.5%, respectively. Strong aspiration of better performance has always been at the central issue of experts [40–46]. Li *et al.* [47] obtained few-layer black phosphorus saturable absorbers with non-saturable absorption of 1% and saturation intensity of 221 MW/cm^2. Sb, a mono-element 2D material, has been reported to generate ultrashort pulse in Tm-doped fiber lasers as SA with the modulation depth of 48% [48]. Wang *et al.* [36] reported a bismuthine-based SA with the saturation intensity of 113 MW/cm^2.

This paper is organized as follows: in section 1, we will give a brief introduction and background on black phosphorus and its analogs. In Section 2, we will introduce the fabrication method of black phosphorus and its analogs. The method of mechanical exfoliation, liquid phase exfoliation and chemical vapor deposition will be elucidated in detail. In Section 3, we will introduce the characterization of black phosphorus and its analogs one by one. In Section 4, we will discuss the performance of black phosphorus and its analogs as saturable absorbers in passively mode-locking fiber lasers working at 1, 1.5, 2, 3 μm. In Section 5, the applications of black phosphorus and its analogs will be elucidated. We described the applications of optoelectronics, electronics, biomedicine and other fields respectively. In Section 6, we will give some conclusions of this paper and several outlooks about black phosphorus and its analogs.

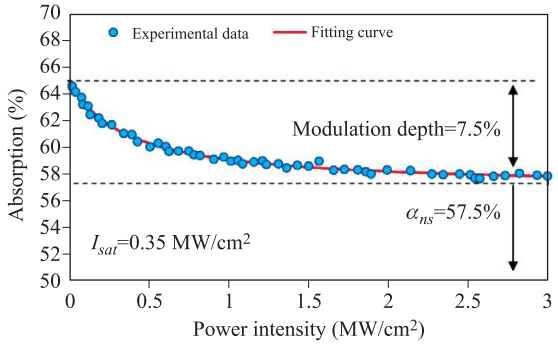

Fig. 1 Nonlinear absorption profile of BP SA. Reproduced with permission from Ref. [39].

2 Fabrication methods of black phosphorus and its analogs

An increasingly number of researchers have paid attentions on the synthesis of black phosphorus and its analogs due to their excellent physical properties and wide application. At present, there are two main fabrication methods, one is called the top-down method, and the other is called the bottom-up method [49–51]. The former includes mechanical exfoliation (ME) [52–54], liquid phase exfoliation (LPE) [27, 43, 55], electrochemicalexfoliation [51, 56], thermal annealing [57], plasma thinning [58, 59] and sonochemical exfoliation method [60–

63]; the latter includes chemical vapor deposition (CVD), pulsed laser deposition [64–67], hydrothermal method [66], van der Waals epitaxy [68, 69] and magnetron sputtering deposition (MSD) [48, 70]. We will briefly introduce three common preparation methods: ME, LPE, and CVD.

2.1 Mechanical exfoliation

Because the layers of two-dimensional layered materials are stacked by inter-planar van der Waals force [9], Novoselov *et al.* [71] found a method to fabricate few-layered crystals through bulk crystals by overcoming the van der Waals force of materials, which is called mechanical exfoliation. Mechanical exfoliation is the process by which bulk crystals are gradually exfoliated into few-layered crystals layer by layer through adhesive tape [72]. It is so convenient that people usually use this method to fabricate black phosphorus in laboratory. However, the defects such as uncontrolled quality and low yield prevent the application of this method in mass production [73, 74]. In addition, even in laboratory scale studies, people cannot effectively control the thickness, size, and shape of the production by this method [72, 75]. Ismail *et al.* [76] fabricated α-In_2Se_3 by ME method and used it as SA of the mode-locked thulium-doped fluoride fiber laser. In order to fabricate a few-layered In_2Se_3, they cut a 1 mm^2 sample out of the In_2Se_3 crystal and then placed the sample between two clear tapes for repeated exfoliation. Fan *et al.* [53] considered the advantages of simple and reliable process of ME and the absence of chemical reactions and expensive laboratory equipment, choosing this method to prepare BP flakes.

2.2 Liquid phase exfoliation

In order to achieve the large-scale exfoliation of BP and its analogs, researchers explored another method named liquid phase exfoliation to prepare them. LPE is a popular method to synthesis saturable absorbers using two-dimensional materials, and its steps are as follows [77]. Firstly, we can destroy the van der Waals forces between the layers of bulk materials in some way such as oxidation, ion intercalation [78] and ultrasonic exfoliation [78, 79]. Then we can use liquid dispersion solvent to transfer the exfoliated material to water by centrifugation. Obviously, the choice of solvent plays a key role in the preparation of materials using this technique. Currently, the commonly used solvents are ethanol [31], NMP (N-methyl-2-pyrrolidone) [72, 79–81], DMF (dimethyl formamide), IPA (isopropanol) [78], PVA (polyvinyl alcohol) [82–84], acetone, and surfactant sodium cholate. For example, Chu *et al.* [79] studied a LPE strategy using NMP to fabricate BP with water stability and controllable layer and dimension. Yu *et al.* [78] explored a novel LPE method, with the assistance of Li_2SiF_6, which combines ion intercalation with ultrasonic treatment to achieve a yield of up to 75%. Zhang *et al.* [85] produced two-dimensional nonlayered Te using IPA as solution through LPE method. Although the yield of LPE method is relatively high, large-scale production is always a problem we are confronted with. After all, ultrasonication is still a laboratory-based process [86].

2.3 Chemical vapor deposition

Chemical vapor deposition (CVD) is a method for large-scale preparation of two-dimensional materials [73], which is often used in integrated electronic devices and transparent electrodes [86]. The preparation of BP using CVD has been extensively studied. The principle of CVD method is that after the material is crushed or even vaporized, solid depositions are generated on the substrate material to form thin films through the redox [52, 87]. Obviously, the certain substrate plays an important role in the preparation using CVD. At present, the substrate materials commonly include Cu, h-BN [64] and Si [87]. Ji *et al.* [87] reported the main process of CVD method and obtained the BP films with average areas >3 μm^2 and ~4 layers. The bottom-up approach allows direct synthesis of 2DLMs at the molecular level, as opposed to the top-down approach. CVD methods are commonly used to directly produce high quality 2DLMs. Because temperature, air pressure and air flow will affect the quality of the few-layered materials prepared by CVD, we can control the quality of film by changing these parameters. In general, the quality of 2DLM prepared by CVD method is higher, but the corresponding cost and complexity are also higher.

2.4 Other methods

In addition to the three methods described above, other methods of preparing black phosphorus and its analogs have been explored by the scientific community [57, 88–92]. As shown in Fig. 2, we introduced several main fabrication methods.

The significant advantages of electrochemical exfoliation are simple, economic and environmentally friendly. Wu *et al.* [93] used the BP as a cathode for electrochemical exfoliation and obtained BP nanosheets with a lower degree of oxidation than the initial material. Through thermal annealing method, Feng *et al.* [94] obtained large transverse sized and defect-free BP flakes and Zhang *et al.* [95] fabricated surface-modified InSe nanosheets with enhanced stability and photoluminescence. Lee *et al.* [58] obtained BP flakes with smooth surface and a designated number of layers using plasma thinning method. This method has the advantages of low temperature, high speed and high efficiency. However, because explosive gases are involved in the process, this method is dangerous and costly [59]. Lau *et al.* [96] reported a method named pulsed laser deposition to fabricate α-BP flakes, which have tunable direct bandgap. Zeng *et al.* [97] successfully synthesized high quality multilayer antimony monocrystals on mica substrate by van der Waals epitaxy. Liu *et al.* [98] used a novel method named "pressure quenching"

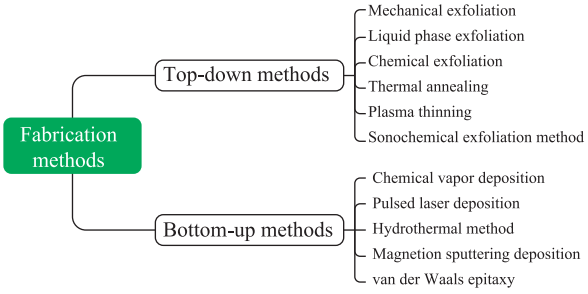

Fig. 2 The fabrication methods of BP and its analogs.

to fabricate BP flakes from red phosphorus through a controllable phase transition under conditions below 0.4 GPa and 580°. Wang *et al.* [99] synthesized Te nanosheets from a culture of a tellurium-oxyanion respiring bacteria.

3 Characterization of black phosphorus and its analogs

In the process from the successful preparation of a new material to the application of this material in the production, the first step is to study the properties of the material. In this section, we will introduce the characterization of black phosphorus and its analogs (including tellurium, selenium, antimony, bismuth, indium selenide, and tin sulfide). At present, the commonly used technical means to explore the properties of materials include high resolution transmission electron microscope (HRTEM), diffraction of X-rays (XRD) and Raman spectrum, etc. HRTEM image can analyze the microstructure of the sample to prove the single crystal properties of the material, XRD diagram can reflect the characteristics of elements and the distribution of atoms in the crystal, and Raman spectrum can analyze the molecular structure.

3.1 Black phosphorus

Phosphorus is widely distributed on earth and is among the top 10 in the earth's crust. Phosphorus has several kinds of allotropes, such as white, red, and black phosphorus. Among them, black phosphorus is the most stable allotrope. BP has four kinds of crystal structure including orthogonal, rhombic, simple cubic and amorphous [100]. At normal temperature and pressure, BP demonstrates a unique orthogonal structure, its space group is Cmca, and the lattice constant is a =4.374 Å, b =3.3133 Å, c =10.473 Å [101]. There are eight phosphorus atoms in each cell of the black phosphorus crystal, and each atom is connected with its three adjacent phosphorus atoms through 3P hybridization orbital. The phosphorus atoms in the same layer are connected by covalent bonds, and the layers are connected by van der Waals forces [72], with an interval of 5.3 Å [81]. Meanwhile, each atom has a lone pair except for the covalent bond, which causes the air instability of BP [102]. Similar to graphene, BP

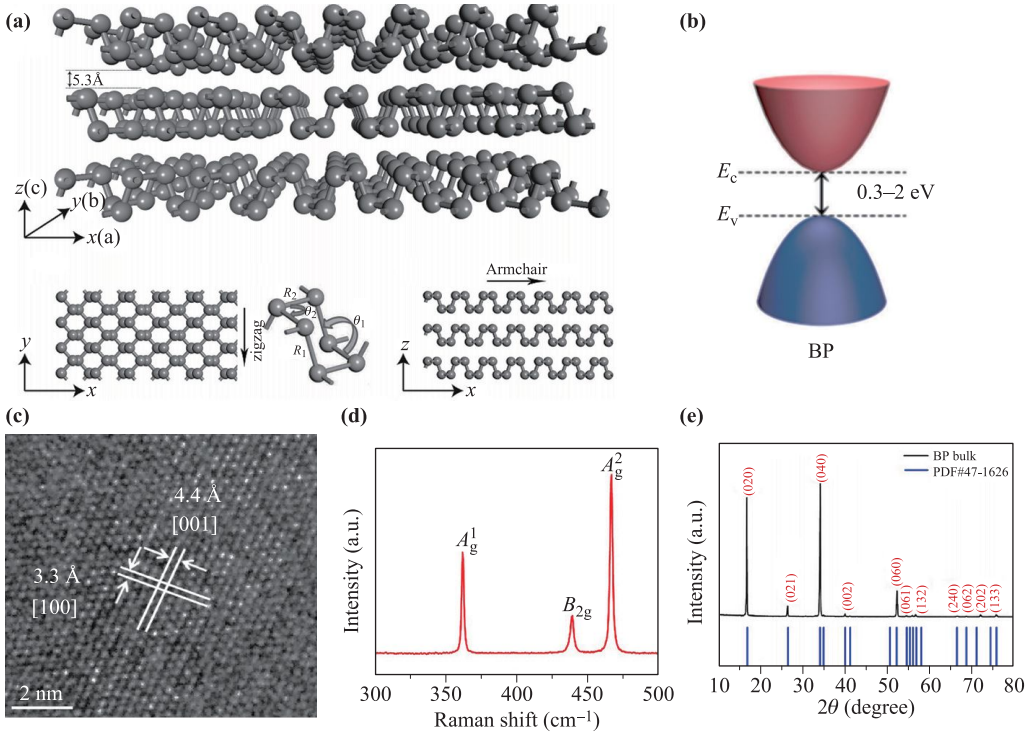

Fig. 3 **(a)** Folded honeycomb structure of BP. **(b)** Schematic diagram of bandgap of BP. **(c)** The HRTEM image of BP. **(d)** Raman spectroscopy of BP. **(e)** The XRD image of BP. Reproduced with permission from Ref. [72] (a), Ref. [111] (b) and Ref. [112] (c–e).

Table 1 The lattice constants of α-Te, β-Te and γ-Te.

α-Te	$a = b = 4.15$ Å
β-Te	$a = 4.17$ Å, $b = 5.49$ Å
γ-Te	$a = b = 3.92$ Å

is a kind of layered material and two-dimensional BP is called phosphoene [103]. However, due to different bond angles (α =96.3°, β =102.1° [104]), the phosphorus atoms in the same layer are not in a plane, but in a folded honeycomb structure, as shown in Fig. 3(a) and thus exhibit strong in-plane anisotropy between the armchair and the zigzag directions [105], as shown in Fig. 3(b). What is even more remarkable is the optical and electrical properties of BP. BP have a direct bandgap depending on thickness as shown in Fig. 3(c) [106, 107]. The bandgap of monolayer, double, triple and bulk black phosphorus are 2 eV, 1.3 eV, 0.8 eV, and 0.3 eV, respectively [105]. The bandgap of BP is the middle of graphene (0 eV) and Transition metal dichalcogenides (TMDCs) (1–2.5 eV) [108, 109]. Furthermore, Jia *et al.* [110] measured 15-nm-thick BP and found its field-effect mobility is up to 205 $cm^2 \cdot V^{-1} \cdot s^{-1}$. Raman spectroscopy is often used to study the molecular constructure of substances. As shown in Fig. 3(d), the Raman spectroscopy of BP clearly illustrate three typical vibration modes, including 361.8 cm^{-1} (A_g^1), 439.2 cm^{-1} (B_{2g}) and 466.8 cm^{-1} (A_g^2).

3.2 Mono-elemental analogs

3.2.1 Tellurene

Tellurium (Te) is one of the Group-VIA elements [113]. At present, as a new two-dimensional single-atom material, it has been used in several field such as field-effect transistors, optical detector and so on. As with other two-dimensional materials, Te has several allotropes, which includes α-Te, β-Te and γ-Te, among them, the first two being semiconductor properties and the latter exhibiting metallic properties [114]. At normal temperatures and pressures, the lattice constants of the three allotropes of Te mentioned above are shown in Table 1. Meanwhile, Te has a triangular lattice structure [100]. There are three Te atoms in each cell of Te crystal. Fig. 4(a)–(c) show the molecular structure of Te and presents us the chain-like structure of Te: each Te atom on the same chain is connected to its two adjacent Te atoms by covalent bond [100]. Therefore, as a non-layered material, Te has strong covalent bond within the chain and shows the Van Der Waals force between the chains, which is different from the inter-layer force of black phosphorus [85]. At the same time, Te has a very strong anisotropy similar to is similar to black phosphorus and other analogs, which makes it have a strong tendency to form one-dimensional nanostructures along the C axis, including Te nanorods, Te nanotubes, Te nanorires, and Te nanoribbons [115]. As shown in Fig. 4(e), the Raman spectroscopy of Tellurene shows three distinct peaks: E_1, A_1, E_2. Unfortunately, there are few studies on Te. In 2017, Zhang *et al.* [114] firstly have been focus on the environmental stability of two-dimensional Te, and they found that Te had a high carrier mobility. In 2019, Xu *et al.* [116] first used Z-scanning technology to explore the broadband nonlinear absorption characteristics of Te.

3.2.2 Antimonene

Antimony (Sb), like bismuth and phosphorus, belongs to the mono-element materials of Group-VA [119]. Antimony

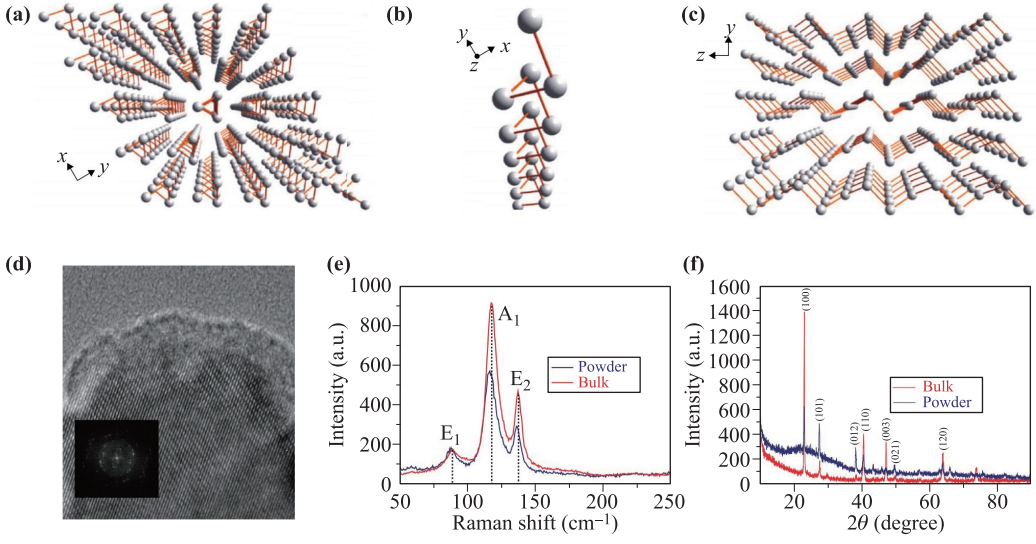

Fig. 4 **(a–c)** Crystal structure of Te viewed from the z axis, as a single-molecule chain, and viewed from the x axis. **(d)** The HRTEM image of Tellurene. **(e)** Raman spectroscopy of Tellurene. **(f)** The XRD image of Tellurene. Reproduced with permission from Ref. [117] (a–c), Ref. [99] (d) and Ref. [118] (e, f).

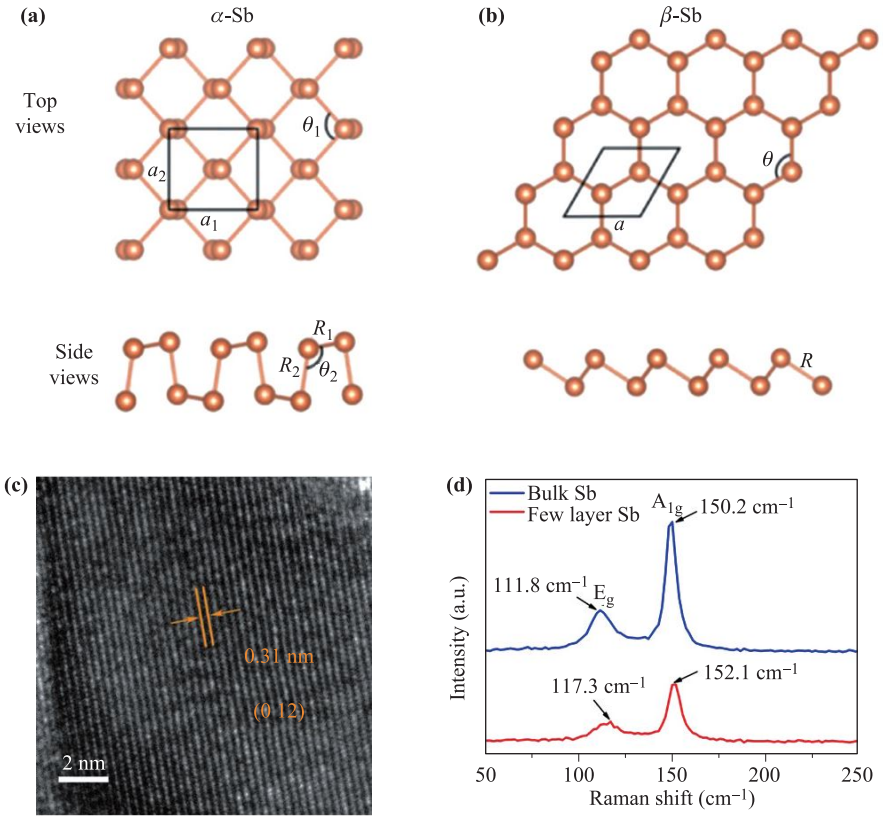

Fig. 5 **(a, b)** The structure of α-Sb and β-Sb. **(c)** The HRTEM image of antimonene. **(d)** Raman spectroscopy of antimonene. Reproduced with permission from Ref. [120] (a–c), Ref. [121] (c) and Ref. [121] (d).

is called the cousin of phosphorus because of its similar structure and properties with phosphorus. Antimony has a dull gray metallic luster, showing a semi-metallic character [100]. According to report, there are four allotropes of antimony [120], among which β-Sb has been well studied because of its excellent stability, and its structure is shown as Fig. 5(b). Meanwhile, Fig. 5(a) shows the structure of α-Sb. Antimony has a bandgap ranging from 0 to 2.28 eV (monolayer) and can change from indirect to direct under biaxial strain [80, 121]. In addition, antimony has a buckled honeycomb structure and exhibits outstanding properties such as strong spin-orbit coupling (SOC), excellent thermal conductivity and high carrier mobility. These excellent properties of antimony have attracted scientists to further study it. Fu *et al.* [122] first implemented dual wavelength mode-locking using antimonene-based saturable absorbers, which was a solid step forward in the application of the generation of Terahertz waves using antimonene. Ruan *et al.* [48] firstly used 2D antimony as SA in ultrafast passively mode-locking fiber lasers working at 1.5 and 2 μm wavelengths.

3.2.3 Bismuthene

Bismuth (Bi) is the last and heaviest element of Group-VA [123]. Bulk bismuth is metallic and diamond-shaped in natural state. Studies have shown that when the number of layers is reduced to below 22, bismuth will show the property of topological insulator; when the number of layers is less than 8, it will show the quantum spin Hall phase, and in the case of single layer Bi shows the property of semiconductor [70]. There are many allotropes of Bi such as α-Bi and β-Bi. Like other materials mentioned in this paper, bismuth atoms are also connected with the three atoms around them through covalent bonds, thus forming a low-buckled honeycomb structure as shown in Figs. 6(a) and (b) [36, 124]. The lattice constant is 4.54 Å, and the Bi-Bi bond length is 3.05 Å [62]. The direct bandgap range of bismuth is from 0 to 0.55 eV [60], filling the gap between graphene and black phosphorus. Compared with black phosphorus, Bi is more difficult to be oxidized in the atmosphere, and has a carrier mobility of several thousand, so it is considered as a more promising optoelectronic material [36].

3.3 Dual-elemental analogs

3.3.1 Indium selenide

Indium selenide is a new kind of two-dimensional sulfide semiconductor with high mobility [126]. By means of X-ray diffraction study, it is found that there are about five dielemental compounds in indium selenide melt, among which InSe and In_2Se_3 have been deeply studied due to

their unique structure [127]. The structure of InSe single crystals is composed of superimposed atomic planes, each of which contains four covalent bond flakes of Se-In-In-Se sequences [128], spaced at 0.83 nm apart. In_2Se_3 is composed of vertically superimposed Se-In-Se-In-Se sandwich structure [129, 130]. Studies have shown that there are at least five crystal types in In_2Se_3 at different temperatures (i.e. α, β, γ, δ, κ). What more interesting is that InSe is the indirect bandgap (bandgap range from 1.2 eV to 1.4 eV) and In_2Se_3 is the direct bandgap. In addition, indium selenide has rhombohedral crystal cells, whose lattice constants are $a = b = 4.05$ Å and $c = 25.32$ Å. As shown in Fig. 7(e), obvious Raman shifts at 115.1, 175.8 and 224.4 cm^{-1} were recorded.

3.3.2 Tin sulfide

Tin sulfide is a monochalcogenide of Group-VA, which has a rhomboid lattice structure similar to that of black phosphorus [131], and its lattice constant is $a = 4.33$ Å, $b = 11.19$ Å, $c = 3.98$ Å [67]. As shown in Fig. 8(b), the HRTEM image shows the interplanar spacing of atoms of tin sulfide in the plane, which are 0.32 nm (210) and 0.30 nm (111). The most distinctive feature of tin sulfide is that it has both direct and indirect bandgaps, ranging from 1.3 eV to 1.6 eV and 1.0 eV to 1.35 eV, respectively. There is only weak van der Waals force and no suspended bond in SnS, so it has a chemically inert surface. This gives it stable chemical properties. Meanwhile, tin sulfide has a better nonlinear absorption coefficient (50.5×10^{-3} cm/GW) than black phosphorus. In addition, the non-toxicity of tin sulfide and abundant reserves of its elements are also great advantages of its large-scale application [132].

4 The performance of black phosphorus and its analogs as saturable absorbers of passively mode-locked fiber lasers

In the previous section, we introduced the properties of black phosphorus and its analogs and found that the analogs are more stable and have a wider adjustable bandgap than black phosphorus, which enables the saturable absorbers made of the analogs to have better stability and wider working ranges. And the advantage of black phosphorus is that it is easier to make. For these reasons, scientists carried out the research simultaneously of black phosphorus and its analogs as saturable absorbers. The scientists focused on the studying of the photoelectric and nonlinear optical properties of black phosphorus and its analogs, such as adjustable bandgap, low saturation strength, fast carrier mobility and small volume, which allow them to be made into saturable absorbers with large modulation depth and flexible operating ranges. It is also worth noting that black phosphorus and its analogs generally have the advantage of being small in size, which makes it easy to be prepared into various forms of saturable absorbers to meet various requirements. Because of their outstanding properties, the passively mode-locked fiber lasers with saturable absorbers made of black phosphorus and its analogs can obtain shorter pulses (up to picosecond and even femtosecond magnitude). Figure 9

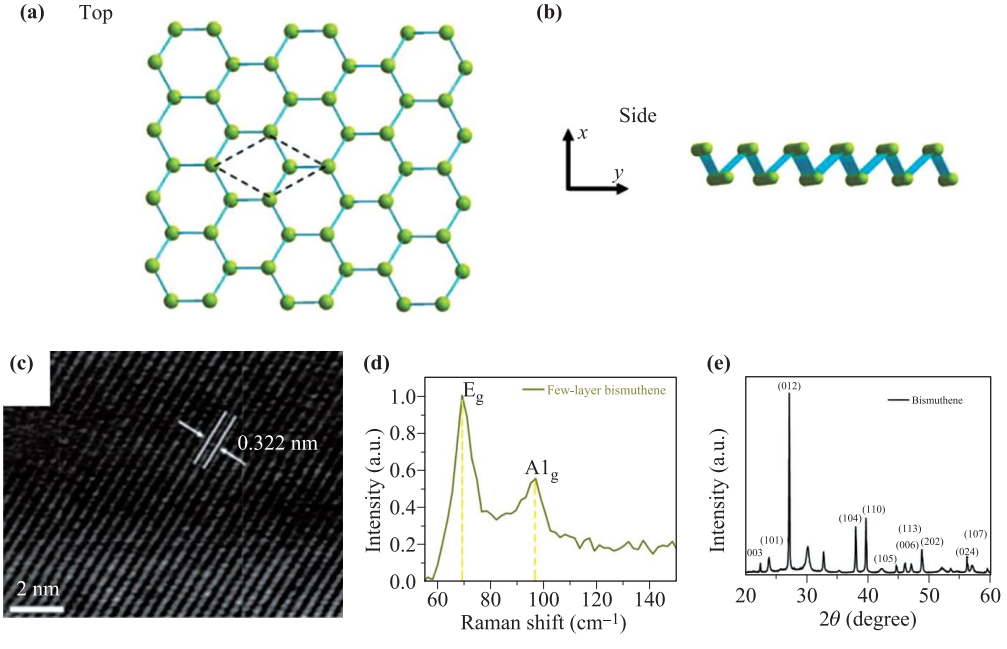

Fig. 6 **(a, b)** Top view and side view of the structure of bismuthine. **(c)** The HRTEM image of bismuthine. **(d)** Raman spectroscopy of bismuthine **(e)** The XRD image of bismuthine. Reproduced with permission from Ref. [125] (a, b), Ref. [124] (c), Ref. [123] (d) and Ref. [63] (e).

shows a typical structure of the passively mode-locked fiber laser using black phosphorus saturable absorber (BP-SA). In this section, we will talk about the performance of passively mode-locked fiber lasers working at different wavelength and using black phosphorus and its analogs as saturable absorbers.

4.1 Working at ~1 μm

Fiber lasers working near 1.0 μm have been widely studied due to their applications in fiber communication, laser guidance, frequency-doubling laser light source and pumping light source [134]. Table 2 shows the performance of passively mode-locked fiber lasers operating at 1 μm and using BP and its analogs as SA. Li *et al.* [47] achieved mode-locking operation at high repetition rate of 46.3 MHz at central wavelength of 1030.6 nm. Zhou *et al.* [135] reported a mode-locked nanosecond fiber laser, which uses BP-SA fabricated by electrochemical delamination exfoliation method, can stably switch the state between of bright and dark pulse. The fiber laser has output power of 8.62 mW in the central wavelength of 1067.1 nm when working at dark pulse state. Harun *et al.* [136] built a Yb-doped fiber laser using BP-SA with output power up to 80 mW. Ge *et al.* [123] obtained the ultrashort pulse with pulse width of 76.62 ps as shown in Figs. 10(a) and (e). Tsang *et al.* [129] explored further applications of α-In_2Se_3 in the field of ultrafast photonics and achieved mode-locking operation of 252 fs in Yb-doped fiber lasers. Its central wavelength, average maximum output power and repetition rate are 1060.6 nm, 2 mW and 14.09 MHz respectively.

4.2 Working at ~1.5 μm

In the past decades, many researchers have been studying the output performance of passively mode-locked fiber lasers working near 1.5 μm, which makes the development of fiber lasers near 1.5 μm more mature [140–145]. 1.5 μm is the optical communication window of quartz fiber [146]. However, it was not until 2015 that high-quality few-layered black phosphorus was successfully prepared and its transmittance was found to increase with light intensity. Researchers began to use black phosphorus and its analogs to make saturable absorbers and apply them in passively mode-locked of fiber lasers. Fortunately, due to the fascinating properties of these two-dimensional materials, the research in this field continues to deepen [18, 147–151]. Table 3 shows main achievements to date in this field.

Recently, in addition to black phosphorus, its analogs have also been reported due to their excellent properties of SA [152–159]. Zhu *et al.* [66] obtained a compact fiber laser with SnS as saturable absorber, and its pulse duration and repetition rate were 1.02 ps and 459 MHz, respectively. Man *et al.* [130] successfully prepared few-layered In_2Se_3 by using physical vapor deposition method and fabricated it as the saturable absorber. By applying it in Er-doped fiber laser, high power output of 121.2 mW is achieved. Hasan *et al.* [79] reported a long-term stable BP-based mode-locked femtosecond fiber laser, its pulse duration of 102 fs as shown in Figs. 10(b) and (f). Their research result is the best performance among all reported mode-locked fiber lasers based on BP and its analogs in the 1.5 μm region and showed that black phosphorus has great potential as an excellent candidate for long-term stable ul-

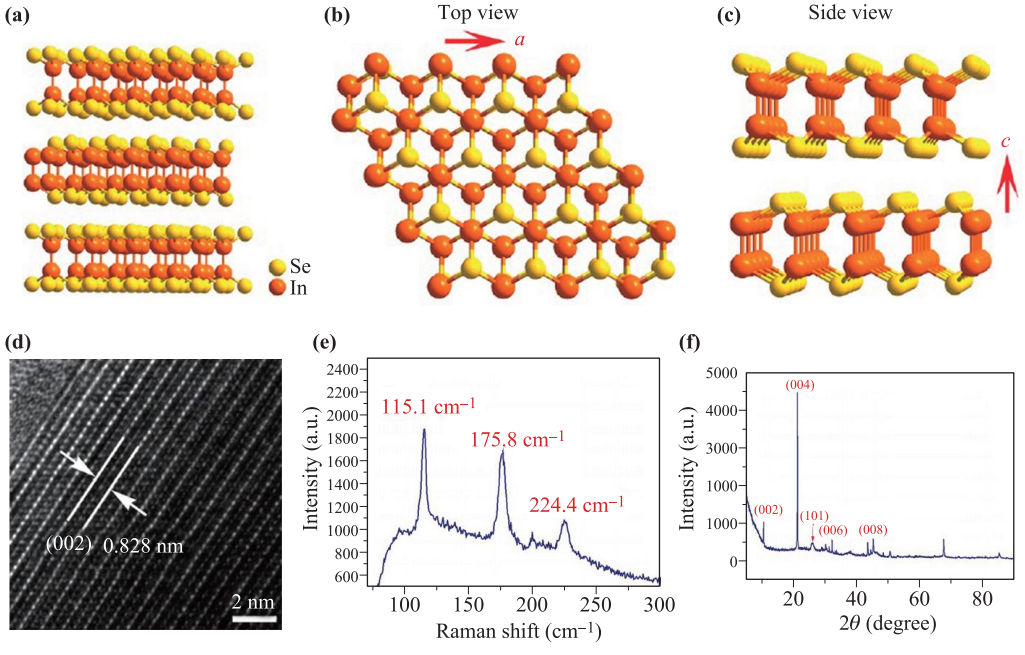

Fig. 7 **(a–c)** The structure of InSe and the top view and side view. **(d)** The HRTEM image of InSe. **(e)** Raman spectroscopy of InSe. **(f)** The XRD image of InSe. Reproduced with permission from Ref. [95] (a–d) and Ref. [83] (e, f).

Table 2 Performance summary of passively mode-locked fiber lasers working 1 μm using BP and its analogs as saturable absorbers.

Materials	Fabrication methods	Gain medium	α_s (%)	I_{sat} (MW/cm^2)	α_{ns} (%)	λ (nm)	t_{min}	Output power	RF (MHz)	Ref.
BP	LPE	Yb	8.5	2.95	1	1030.6	5 ps	—	46.3	[47]
BP	ME	Yb	7.5	0.35	57.5	1033.76	3.27 ps	—	10	[39]
BP	electrochemic–al delamination exfoliation	Yb	—	—	26.1	1063.3	386.3 ns	2.63	0.39	[135]
BP	LPE	Yb	12.5	27.9	—	1064.6	51 ps	—	—	[134]
BP	electrochemic–al delamination exfoliation	Yb	—	—	26.1	1067.1	68.4 ns	8.62	0.39	[135]
BP	ME	Yb	8	0.35	57	1085.58	7.54 ps	80	13.5	[136]
Bismuthene	sonochemical exfoliation	Yb	2.2	13	—	1034.4	30.25 ps	—	21.74	[63]
Bismuthene	—	Yb	1	2.4	—	1035.8	—	—	21.74	[123]
α-In_2Se_3	LPE	Yb	—	—	—	1060.6	252 fs	2	14.09	[129]
InSe	LPE	Yb	4.2	15.6	—	1068.36	1.37 ns	16.3	1.76	[84]

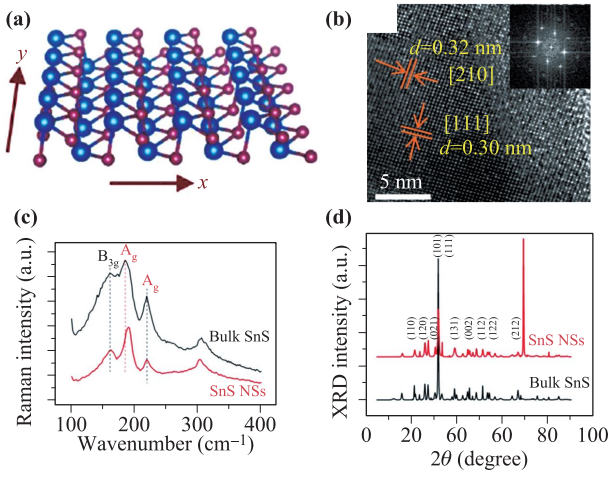

Fig. 8 **(a)** The structure of SnS. **(b)** The HRTEM image of SnS. **(c)** Raman spectroscopy of bulk SnS and SnS nanosheets (SnS NSs). **(d)** The XRD image of SnS. Reproduced with permission from Ref. [131] (a), and Ref. [133] (b–d).

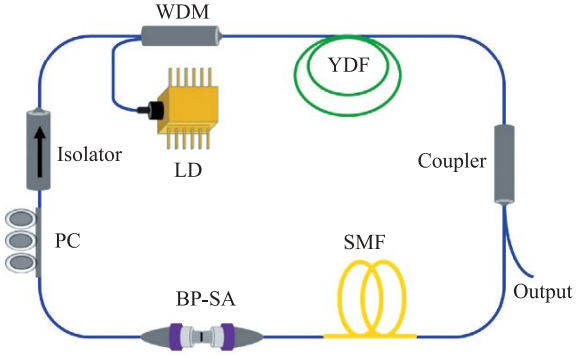

Fig. 9 The schematic of passively mode-locked Er-doped fiber laser using BP-SA. Reproduced with permission from Ref. [39].

trashort pulse generation. Zhao *et al.* [152] and Zhang *et al.* [151] obtained wavelength tunable ultrafast fiber lasers from 1529 nm to 1592 nm and 1549 nm to 1575 nm, respectively. Their study provides an effective solution for the application of the infrared or mid-infrared ultrafast fiber laser which is widely tunable.

4.3 Working at ~2 μm and ~3 μm

The fiber lasers operating near 2 μm most use thulium as the gain medium. Meanwhile, it is safe for human eyes, the 2 μm laser thus widely used in meteorological monitoring, laser ranging, lidar, remote sensing and other fields [165]. In addition, water molecules near 2 μm has a strong mid-infrared absorption peak, the surgery using this band laser is conducive to speed up blood coagulation and reduce surgical trauma. Mid-infrared fiber laser in the medical and life sciences has an important application. Abramski *et al.* [161] first reported a thulium-doped fiber laser using BP-SA and obtained 739 fs mode-locked pulse. Yang *et al.* [160] used MSD method to make α-In_2Se_3 into a saturable absorber with broadband saturation absorption characteristics, and they applied it to a passively mode-locked fiber laser to obtain a mode-locked pulse with pulse width of 1020 fs and output power of 112.4 mW. In addition, Nie *et al.* [162] used liquid phase peeling technique to produce a novel chemically synthesized tellurium thin film (Chem-Te) and first reported its saturable absorption characteristics in a 2 μm fiber laser. Figures 10(c) and (g) show the optical spectrum and autocorrelation trace of fiber laser working at ~2 μm measured by Jiang *et al.*

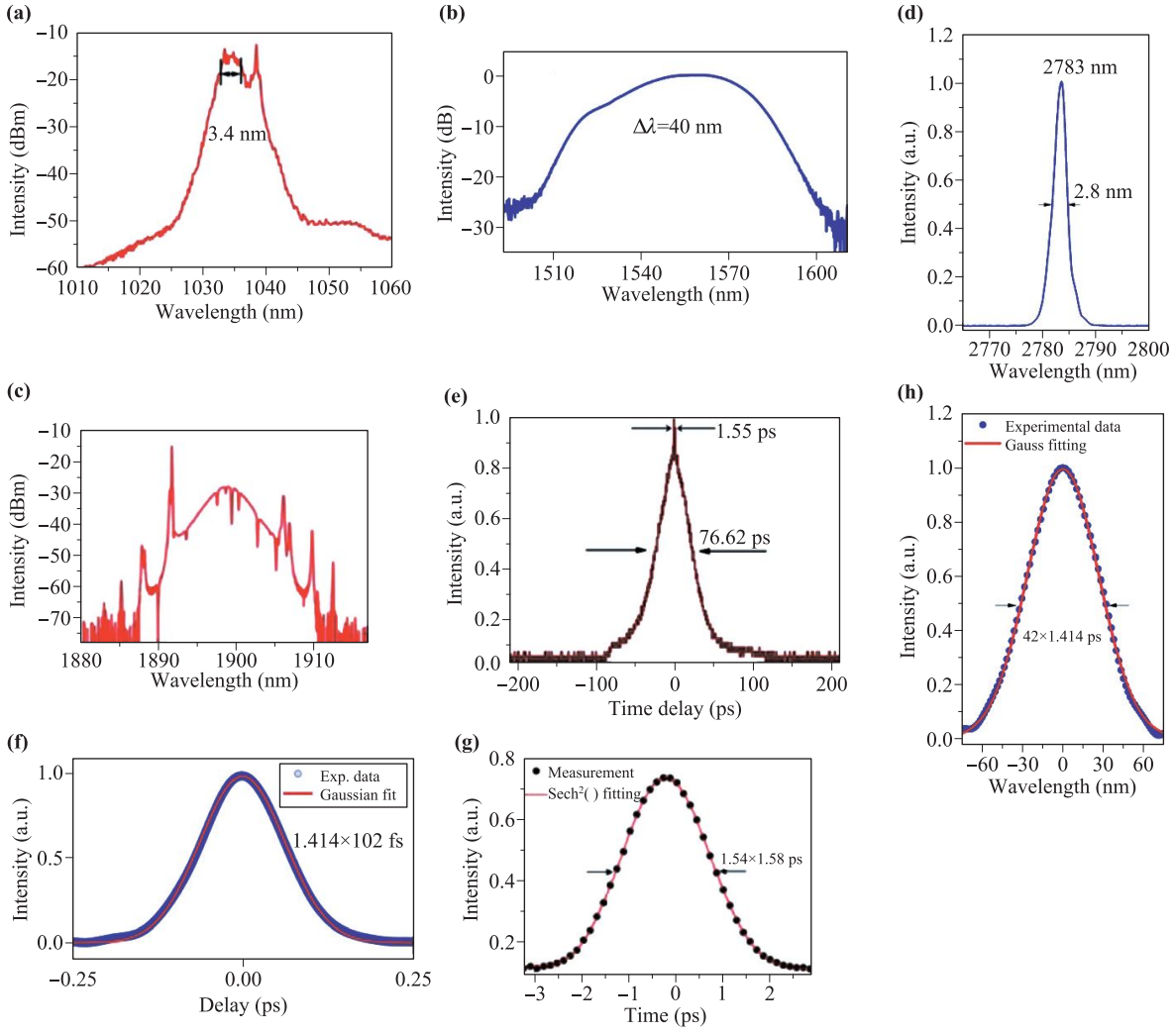

Fig. 10 **(a–d)** Optical spectrum of fiber lasers working at 1, 1.5, 2, 3 μm, respectively. **(e–h)** Autocorrelation trace of fiber lasers working at 1, 1.5, 2, 3 μm, respectively. Reproduced with permission from Ref. [123] (a), Ref. [137] (b), Ref. [138] (c), Ref. [139] (d), Ref. [123] (e), Ref. [137] (f), Ref. [138] (g) and Ref. [139] (h).

Fiber lasers working at ~3 μm have potential applications in biological, medical and other fields. Meanwhile, these lasers can also be used as pumping light source for medium and far infrared laser. Fluoride glass is generally as the fiber substrate of the passively mode-locked fiber lasers working at ~3 μm because the laser emission near 3 μm requires the substrate material to have low phonon energy and high optical head pass rate. Shen *et al.* [164] first applied saturable absorber made of black phosphorus in an erbium-doped fiber laser in the region of 3 μm, and obtained a pulse width of 213 fs. At the same time, the output power of the laser could reach 40 mW. Qian *et al.* [139] used ME method to prepare multilayer black phosphorus and applied it to ultrafast fiber laser, obtaining the maximum average output power of up to 613 mW as shown in Figs. 10(d) and (h). Liu *et al.* [163] used the co-doped Ho^{3+}/Pr^{3+} fluoride fiber as the gain medium and black phosphorus as the saturable absorber to obtain the passively mode-locked output, which has pulse width of 8.6 ps, output power of 87.8 mW and repetition rate of 13.987 MHz. Table 4 shows data we collected about the performance of the fiber lasers working at 2 and 3 μm.

5 Applications of black phosphorus and its analogs

At present, black phosphorus and its analogs are widely used in many fields [102], such as photodetector, optical modulators, solar cells, transistors [208], electrochemical energy storage devices, piezoelectric devices [117], as well as in drug delivery, bioimaging, photothermal therapy, photodynamic therapy, photocatalyst and sensors, as shown in Fig. 11. Of course, this is due to their excellent material properties. For example, BP is suitable for photodetector [27] because it has a strong impact to

Table 3 Performance summary of passively mode-locked fiber lasers working ~1.5 μm using BP and its analogs as saturable absorbers.

Materials	Fabrication methods	Gain medium	α_s (%)	I_{sat} (MW/cm^2)	α_{ns} (%)	λ (nm)	t_{min}	Output power	RF (MHz)	Ref.
BP	LPE	Er	10.03	14.98	9.97	1555	102 fs	—	23.9	[137]
BP	water-exfoliated method	Er	1	221	—	1557.8	1.2 ps	—	6.317	[140]
BP	—	Er	3.31	12.5	73.6	1558.14	2.18 ps	—	15.59	[141]
BP	—	Er	—	—	—	1558.7	786 fs	—	14.7	[142]
BP	LPE	Er	0.35	—	—	1558	700 fs	1.5	20.82149	[143]
BP	LPE	Er	21.00	12	40	1559.5	670 fs	—	~8.77	[144]
BP	ME	Er	7.00	0.25	58	1560.7	570 fs	5.1	6.88	[145]
BP	ME	Er	7.75	—	10	1560	580 fs	—	15.2	[147]
BP	LPE	Er	0.8	—	—	1561	1.438 ps	—	5.268	[18]
BP	ME	Er	6.90	0.25	—	1561	2.66 ps	—	1	[148]
BP	LPE	Er	~ 0.3	—	—	1562	1.236 ps	—	5.426	[18]
BP	—	Er	—	—	—	1564.6	690 fs	—	3.47	[149]
BP	LPE	Er	10.90	25	—	1566.5	940 fs	5.6	4.96	[150]
BP	ME	Er	8.10	6.55	—	1571.45	946 fs	—	5.96	[53]
BP	LPE	Er	10	8.3	—	1576.1	403.7 fs	1.9	34.27	[134]
BP	LPE	Er	10.1	9.27	—	tunable	280 fs	—	—	[151]
BP	LPE	Er	0.76	5.1	22.64	tunable	0.9 ps	—	5.65	[152]
BPQDs (black phosphorus quantum dots)	LPE	Er	8.10	—	—	1561.7	0.88 ps	—	5.47	[153]
BPQDs	LPE	Er	9	1.5	—	1562.8	291 fs	—	10.36	[154]
BPQDs	solvothermal synthesis	Er	36	3.3 GW·cm^{-2}	—	1567.5	1.08 ps	—	15.25	[155]
Tellurene	LPE	Er	11.86	44.65 GW·cm^{-2}	—	1556.57	879 fs	3.45	15.45	[115]
Tellurene	LPE	Er	10.5	26 GW·cm^{-2}	—	1556.57	879 fs	3.45	15.45	[115]
Tellurene	LPE	Er	27	78.14 GW·cm^{-2}	—	1556.57	879 fs	3.45	15.45	[115]
Tellurene	LPE	Er	35.64	1.06	25.91	1558.8	1.03 ps	3.69	3.327	[156]
Tellurene	LPE	—	5.06	34.3	—	1563.97	38.5 ps	106.6	12.17	[118]
Tellurene	LPE	Er	0.97	—	42.30	1565.58	21.45 ps	17.44	5.0378	[82]
Tellurene	LPE	—	5.06	34.3	—	1573.97	5.87 ps	23.61	12.17	[118]
Antimonene	vapor deposition	Er	11.77	9.17	—	1562.64	753 fs	—	—	[157]
Antimonene	MSD	Er	25	28	—	1557	544 fs	21.76	17.15	[48]
Antimonene	LPE	—	3.96	14.25 GW·cm^{-2}	—	1557.68	552 fs	—	10.27	[80]
Antimonene	LPE	—	19.72	15.10 GW·cm^{-2}	—	1557.68	552 fs	—	10.27	[80]
Bismuthene	LPE	Er	7.7	16	—	1530.4	1.75 ps	—	4	[158]
SnS	sol-hydrothermal method	Er	5.4	66.3	—	1530.6	1.29 ps	—	5.47	[65]
Bismuthene	LPE	Er	2.5	113	66.3	1531	1.303 ps	—	4	[36]
Bismuthene	—	Er	2.5	110	—	1555.7	—	—	4	[159]
Bismuthene	sonochemical exfoliation method	Er	2	0.3	—	1557.5	621.5 fs	—	22.74	[62]
Bismuthene	sonochemical exfoliation method	Er	2.03	30	—	1559.18	652 fs	—	8.83	[61]
Bismuthene	sonochemical exfoliation method	Er	5.60	48.2	62.3	1561	193 fs	5.6	8.85	[60]
α-In_2Se_3	ME	Tm	14.6	0.4 kW/cm^2	—	1503.8	5.79 ps	1.242	6.98	[76]
α-In_2Se_3	LPE	Er	—	—	—	1550	215 fs	2	7.31	[129]
In_2Se_3	PVD	Er	18.75	6.8	18.89	1559.4	14.4 ns	122.4	1.71	[130]
α-In_2Se_3	LPE	Er	—	—	—	1560.08	215 fs	2	7.31	[129]
α-In_2Se_3	MSD	Er	4.5	7.3	21.9	1565	276 fs	83.2	40.9	[160]
SnS	LPE	—	36.40	~34.8 GW·cm^{-2}	27.7	1560	656 fs	—	8.37	[133]
SnS	hydrothermal method	Er	5.8	52.2	~35	1562.4	1.02 ps	—	459	[66]

the photon from near ultraviolet to infrared wavelengths. SnS has great application potential in the solar cells and other optical devices because its bandgap is close to the best forbidden band width of solar cells.

Table 4 Performance summary of passively mode-locked fiber lasers working 2 μm and 3 μm using BP and its analogs as saturable absorbers.

Materials	Fabrication methods	Gain medium	α_s (%)	I_{sat} (MW/cm^2)	α_{ns} (%)	λ (nm)	t_{min}	Output power	RF (MHz)	Ref.
BP	ME	Tm	9.8	—	78.1	1898	1.58 ps	—	19.2	[138]
BP	ME	Tm	4.1	—	52.2	1910	739 fs	1.5	36.8	[161]
Chem-Te	LPE	Tm	13.71	80.7	32.09	1971	890 fs	5.35	11.17	[162]
Antimonene	MSD	Tm	48	32	—	1892	972 fs	36.1	15.5	[48]
α-In_2Se_3	MSD	Tm	6.9	10.6	28.8	1932	1020 fs	112.4	15.8	[160]
BP	ME	Er	19	—	—	2783	42 ps	613	24	[139]
BP	LPE	Ho^{3+}/Pr^{3+}	41.20	3.767	7.6	2866.7	8.6 ps	87.8	13.987	[163]
BP	—	Er	7.70	—	14	3489	213 fs	40	28.91	[164]

5.1 Optoelectronic characteristics

We believe that the application of black phosphorus and its analogs in the field of optoelectronics is worthy of the attention from scientific community [166]. And the photodetector is very representative in this field [167]. The photodetector is a device that converts optical signals into electrical signals, which has a wide range of applications in daily life, including environmental monitoring, medical imaging, optical communication, security and military applications [168]. Two-dimensional materials such as black phosphorus generally have strong photomaterial interactions, making them promising candidates for high performance photodetector applications. Ozyilmaz *et al.* [169] proved that black phosphorus is an excellent material for ultraviolet photodetectors with specific detectivity up to 3×10^{13} Jones. Photodetectors made of black phosphorus and its analogs have excellent performance, including ultrabroad detecting band, ultrahigh light absorption efficiency and fast photo-response. Studies have shown that black phosphorus and its analogs have a wide detection band from near ultraviolet to longwave infrared [170]. Two-dimensional layered materials such as black phosphorus and its analogs interact strongly with photon. The quantum constraint of vertical direction leads to a spike in the state density near the edge of the conduction and valence band, which increases the possibility of excited free electron-hole pairs when the energy of the incident photon approaches the band gap, resulting in higher photon absorption [171]. Cai *et al.* explored the difference in photon absorption between the two crystal axes caused by the anisotropy of black phosphorus and its analogs, and for BP of 70 nm, the light absorption varies between 40% and 10% from the armchair direction to the zigzag direction [172]. BP showed a wide and rapid response from the visible region to the near-infrared region [173]. Buscema *et al.* [174] found that the photodetector made of few-layered black phosphorus showed a response to the wavelength from the visible region to 940 nm and the rise time of about 1 ms, which proved its broadband and rapid detection, and its responsivity reached 4.8 mA/W. Due to the weak interlayer forces of two-dimensional materials, the lattice mismatch requirements between different two-dimensional materials are lower than those of conventional semiconductor heterojunctions. Bao *et al.* [175] reported a graphene-BP heterostructure photodetector, which shows long-term stability and ultra-high photon response (3.3×10^3 AW^{-1}) at near-infrared wavelength (1550 nm). Zhang *et al.* [176] fabricated the Te_x@Se_y with roll-to-roll nanotubes heterojunctions by epitaxial growth of Se on the Te nanotubes and firstly applied it to the photodetectors. Javey *et al.* [177] found people can increase absorption in semiconductors using Al_2O_3/Au optical cavity substrate and make photodetectors using Te by this way. They measured the peak responsiveness of Te photoconductor when the thickness of Al_2O_3 was 550 nm, 150 nm and 350 nm respectively, and this parameter changed from 13 to 8 A/W. Therefore, it was concluded that the performance of photodetectors made by Te could be changed through changing the thickness of the Al_2O_3/Au optical cavity substrate.

In addition to photodetectors, optical modulators are also important optoelectronic devices [178]. Black phosphorus is easy to manufacture high performance all-optical modulators due to their excellent nonlinear optical properties. At present, the BP-based optical modulator mainly uses the Stark effect and the Pauli blocking effect, the former can effectively reduce the bandgap under the vertical electric field, while the latter can transfer the absorption edge to a higher energy [179]. Zhang *et al.* [180] investigated an all-optical modulator using phosphoene that utilizes a Mach-Zehnder interferometer and achieves stability under environmental conditions. Helmy *et al.* [181] demonstrated that a BP-based optical modulator can achieve better maximum absorbability and power efficiency than graphene.

In addition, as solar energy is the new clean and environmentally friendly energy, people try to use two-dimensional materials to make solar cells, so as to make better use of solar energy [182, 183]. Solar cells are devices that convert light energy directly into electricity through the optoelectronic or photochemical effect. Syed Mubeen *et al.* [184] believed that SnS thin films could be used as

an effective photocathode with the maximum photocurrent density up to 12 $mA{\cdot}cm^{-2}$. Shapter *et al.* [185] and Blom *et al.* [186] summarized the current research status on solar cells of black phosphorus. Yu *et al.* [187] carried out a research on improving the performance of solar cells. They combined the photocathode based on BPQDs (black phosphorus quantum dots) into DSSCs (Dye sensitized solar cells), which increased the electron density of DSSCs and improved the electron transport performance of DSSCs. Compared with photoanode of TiO_2 films, Chu *et al.* [188] enhanced optoelectronic conversion of 38% using BP/TiO_2 composites.

5.2 Electronics

In the field of modern electronics, the transistor, as an indispensable basic unit of integrated circuit, has been widely studied. BP and its analogs are considered excellent materials for making transistors [194, 195]. Because they all have a limited bandgap, which allows the transistors they make to have a high pass ratio. Wu *et al.* [22] reported a field-effect transistor (FETs) made by Te, which had good air stability, an on/off ratio of up to 10^6, and a field effect mobility of about 700 $cm^2{\cdot}V^{-1}{\cdot}s^{-1}$, and shown another transistor with the conduction density of 1 $A{\cdot}mm^{-1}$. Lu *et al.* [194] studied the performance limits of single-layer BP Schottky barrier transistors below 10 nm using *ab initio* quantum transport simulations for the first time. Hao *et al.* [125] explored the feature of p-type field-effect transistors by studying the Bi-film FETs, which have the large carrier mobility of 220 $cm^2{\cdot}V^{-1}{\cdot}\,s^{-1}$. Two-dimensional materials such as BP and its analogs have high elasticity and flexibility, which makes them suitable for flexible electronic products. Based on this development prospect, we can foresee that the flexible research of transistors made from these materials will have a broad prospect.

Electrochemical energy storage devices (EESDs) are the device for converting chemical energy into electrical energy. Because their structure is simple, easy to carry, easy to charge and discharge operation, not affected by the outside climate and temperature, stable and reliable performance, in the modern social life in all aspects play a great role [196–198]. The flexibility, large surface area and good electrical conductivity of BP and its analogs make them a promising electrode material of EESDs [72]. Koratkar *et al.* [189] attempted to insert the phosphorus nanosheets into the cathode matrix of lithium sulfur battery to significantly improve the cycle life of lithium sulfur battery and improve the utilization rate of sulfur in the battery. Xiu *et al.* [199] summarized and analyzed the latest research results of black scale and other materials as the positive pole of lithium-based lithium batteries. Guo et al. [200] enhanced the properties of sodium ion batteries, such as structural stability and cyclic stability, by conducting structural phase transition in SnS. Yun *et al.* [201] applied SnS nanoparticles to the anode of the Na^+ battery, and found that the specific energy, power value and first Coulombic efficiency were ~256 $Wh{\cdot}kg^{-1}$,471 $W{\cdot}kg^{-1}$, 90%, respectively.

5.3 Biomedicine

In the field of biomedicine, 2D materials have potential applications in photothermal therapy, photodynamic therapy, bioimaging, drug delivery and so on [202]. For example, BP can produce high photothermal conversion efficiency and thus can be used as a photosensitizer in photothermal therapy and photodynamic therapy [203]. By processing 2D materials to the nanometer level and making nanometer probes, they can be used for multipeak imaging of tumors [204]. BP have certain antibacterial properties and can be used as a clinical platform for against bacteria [191]. Due to the limited space, we mainly present the application status of BP and its analogs in drug delivery.

2D materials have the properties of high drug loading because of their large surface area. Furthermore, 2D BP has low cytotoxicity [205] and degradability, making it an ideal drug delivery platform [21]. A good drug delivery system enables drugs to be released more intensively and efficiently at the target location, significantly reducing the side effects of drugs and improving the efficiency of drug [203]. Kim *et al.* [206] assembled Au and γ-Fe_2O_3 nanoparticles on BP nanosheets (BP-NSs) to develop a biocompatible composite material, the property that enables this material to be used for drug delivery. Zhang et al. [207] summarized the latest advances in medical diagnosis and treatment of few-layered BP. Mei *et al.* [190] prepared BP nanosheets by ME method, then used polyethylene glycol–amine (PEG-NH_2) to improve their biocompatibility and physiological stability, and proved that the drug delivery platform they developed could effectively load doxorubicin (DOX) and cyanine7 (Cy7). Their study shows the medical properties of PEGylated BP-NSs for the first time and the feasibility of using BP nanosheets for medical treatment.

5.4 Other fields

BP and its analogs are not only widely used in the fields mentioned above, but considered ideal and attractive materials in many fields in fact. For example, BP are also used as optical Kerr converters and wavelength converters based on four-wave mixing [105] in the field of optics. We certainly can't go into details here, but we want to present as many of the hottest aspects of current research as we can.

We think what should be paid attention to is the application of black phosphorus as the photocatalyst. Based on the light collected, black phosphorus produces electron-hole pairs that can redox some substance such as water.

Majima *et al.* [208] reported that black phosphorus flakes promoted the release of H_2 in water decomposition reactions, with apparent quantum efficiencies of 8.7% and 1.5% under visible (420 ± 5 nm) and near-infrared light (780 ± 5 nm), respectively. Yu *et al.* [192] prepared a kind of nanocomplexes consisting of black phosphorus and graphitic carbon nitride (CN). They placed BP/CN in water containing IPA to produce hydrogen at a release rate of 786 $\mu mol \cdot h^{-1} \cdot g^{-1}$. At the same time, they further explored the photocatalytic principle of BP/CN. Wang *et al.* [209] summarized the latest progress of BP/CN in photocatalysis. Compared with black phosphorus, this hybrid has better light collection ability and photocatalytic performance. Yang *et al.* [210] summarized some common performance improvement methods for two-dimensional material catalysts such as black phosphorus.

Black phosphorus and its analogs also show unique advantages in sensor applications. Due to their large surface volume ratio and environmental sensitivity, they have been widely used in gas sensors, biosensors and humidity sensors [211]. Rong *et al.* [211] summarized the current application status and future prospects of black phospho-

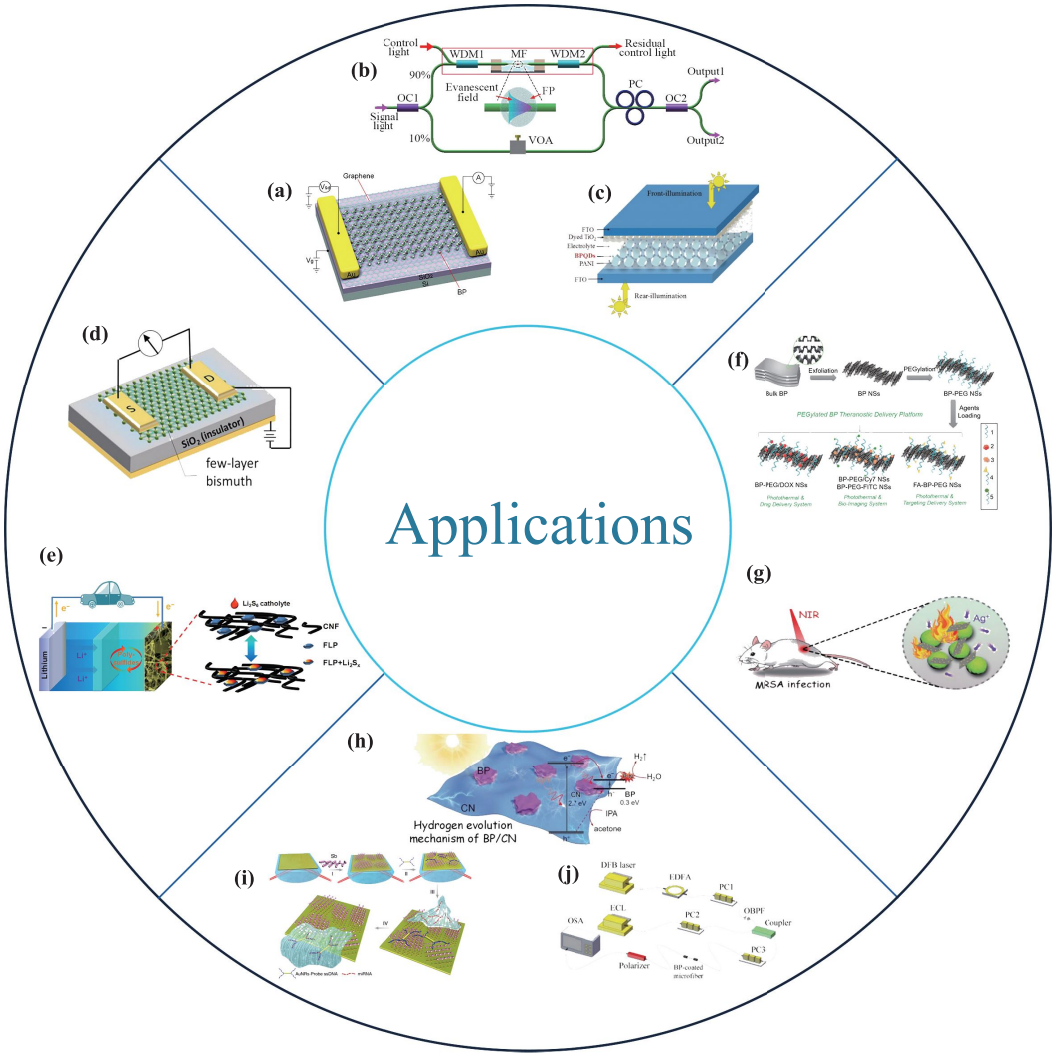

Fig. 11 **(a)** Three-dimensional schematic diagram of the graphene-BP heterostructure photodetector. **(b)** Experimental setup of the Mach-Zehnder interferometer-based all-optical modulator. **(c)** The schematic of the bifacial n-type dye-sensitized solar cell with BPQDs (black phosphorus quantum dots). **(d)** The schematic of FETs based on Bi film. **(e)** Schematic of the few-layer phosphorene and carbon nanofiber matrix used as the host for the lithium polysulphide catholyte. **(f)** Schematic representation of the PEGylated BP theranostic delivery platform. 1: PEG-NH_2 (surface modification), 2: DOX (therapeutic agents), 3: Cy7-NH_2 (NIR imaging agents), 4: folic acid-PEG-NH_2 (targeting agents), 5: fluoresceine isothiocyanate-PEG-NH_2 (fluorescent imaging agents). **(g)** the schematic of synergistic antibacterial effect. **(h)** Schematic of the charge transfer process and mechanism of photocatalytic H_2 emission. **(i)** The process of a Sb-based miRNA sensor fabrication and detect miRNA use it. **(j)** The schematic of Kerr switch. Reproduced with permission from Ref. [175] (a), Ref. [180] (b), Ref. [105] (c), Ref. [125] (d), Ref. [189–193] (e–i) and Ref. [105] (j).

rus in the field of sensors. Bao *et al.* [142] explored the application of Sb-based sensors in MicroRNA detection. Its detection limit is 2.3–10,000 times higher than existing sensors, providing a better choice for cancer diagnosis and detection. There is no doubt that these materials' high sensitivity, repeatability and stability pave the way for industrial applications, safety equipment and health sensing.

6 Conclusion and outlook

As we introduced above, black phosphorus and its analogs have excellent properties, and some achievements have been made on their research [23, 206, 212–214]. But from our perspective, the following issues still need to be tackled in the future:

(i) In terms of preparation method, the existing methods have various problems, for example, the yield of monolayer material prepared by ME is low. LPE method will introduce internal or external defects into 2D materials, which will adversely effect on the application in the next step. And researchers have not yet found the most suitable substrate material of CVD. Meanwhile, although each method claims to be able to produce a controlled thickness of black phosphorus, researchers cannot obtain black phosphorus at the designated thickness. Therefore, how to improve the existing preparation methods or find other more suitable preparation methods will be researchers' future works.

(ii) As described above, black phosphorus is easily oxidized and environmentally unstable. If it is exposed to air, its surface will be corroded layer by layer. Although the degradability of black phosphorus is an advantage in medical applications, in other fields, especially in optics, when researchers use BP as saturable absorbers to generate passively mode-locked pulses, they want the black phosphorus to be more stable so that they can get the steady pulse. Therefore, the preparation of black phosphorus with high stability is also a major research direction [215]. At present, there are two main ways to overcome the degradability of BP, one is surface modification, the other is surface coating [215, 216]. However, the research on the degradation mechanism of black phosphorus caused by environment is still in its infancy. Therefore, the research on the anti-degraded BP is only in the initial stage. In the future, researchers need to go further.

(iii) In the material family of black phosphorus and its analogs, researchers find that the properties of black phosphorus have been extensively studied and revealed, but the study of analogs is still in its early stages, especially many questions remain to be solved in the field of application. Because scientists have studied the properties of 2D black phosphorus deeply, the research on its application is far ahead of its analogs. In the future work, researchers should continue to explore the properties, preparation methods and applications of black phosphorus analogs.

(iv) Heterogeneous structures based on two-dimensional layered materials usually have better performance than single two-dimensional layered materials [22, 168, 217–221]. At the same time, the heterostructure can also be an ideal saturable absorber for pulsed lasers [222]. Therefore, researchers can try to study heterogeneous integration of black phosphorus and its analogs in order to obtain precisely designed van der Waals heterostructures and thus build more powerful devices such as high-power lasers, high-electron-mobility transistors and bipolar transistors [101].

In this review, we have reviewed preparation methods, material properties, current applications of black phosphorus and its analogs, and the performance of them as saturable absorbers in passively mode-locked fiber lasers. We focus on showing their properties as saturable absorbers in lasers working at different central wavelength, which are demonstrated by the pulse generated by the lasers. As we have seen, passively mode-locked pulse outputs from 1 μm to 3 μm can be achieved using black phosphorus and its analogs as SA. At the same time, we can also notice that BP and its analogs, especially BP, are widely used in industry, medical treatment and other fields. With the development of materials science, we firmly believe that the properties of 2D BP and its analogs will be further discovered, they will be ideal SA and will be wider application in various fields.

Acknowledgements We acknowledge the financial support by the China Postdoctoral Science Foundation (No. 2019M651203), Science and Technology Project of the 13th Five-Year Plan of Jilin Provincial Department of Education (Nos. JJKH20190157KJ and JJKH20190169KJ), Jilin Province Science and Technology Development Plan Project (No. 20190201128JC), and Changchun Science and Technology Plan Project (No. 18SS008).

References

1. G. Wang, A. A. Baker-Murray, and W. J. Blau, Saturable absorption in 2D nanomaterials and related photonic devices, *Laser Photonics Rev.* 13(7), 1800282 (2019)
2. C. Wang, J. Liu, and H. Zhang, Ultrafast pulse lasers based on two-dimensinal nanomaterials, *Acta Physica Sinica* 68(18), 188101 (2019)
3. X. Chen, Z. Zhou, B. Deng, Z. Wu, F. Xia, Y. Cao, L. Zhang, W. Huang, N. Wang, and L. Wang, Electrically tunable physical properties of two-dimensional materials, *Nano Today* 27, 99 (2019)
4. L. Yang, W. Chen, Q. Yu, and B. Liu, Mass production of two-dimensional materials beyond graphene and their applications, *Nano Res.* (2020)
5. T. Feng, X. Li, P. Guo, Y. Zhang, J. Liu, and H. Zhang, MXene: Two dimensional inorganic compounds, for gen-

eration of bound state soliton pulses in nonlinear optical system, *Nanophotonics* 9(8), 2505 (2020)

6. P. Cheng, Y. Du, M. Han, and X. Shu, Mode-locked and Q-switched mode-locked fiber laser based on a ferroferric-oxide nanoparticles saturable absorber, *Opt. Express* 28(9), 13177 (2020)
7. M. Paillet, R. Parret, J. L. Sauvajol, and P. Colomban, Graphene and related 2D materials: An overview of the Raman studies, *J. Raman Spectrosc.* 49(1), 8 (2018)
8. Z. Y. Li, Nanophotonics in China: Overviews and highlights, *Front. Phys.* 7(6), 601 (2012)
9. W. Liu, M. Liu, X. Liu, X. Wang, H. X. Deng, M. Lei, Z. Wei, and Z. Wei, Recent advances of 2D materials in nonlinear photonics and fiber lasers, *Adv. Opt. Mater.* 8(8), 1901631 (2020)
10. S. Tang, Z. He, G. Liang, S. Chen, Y. Ge, D. K. Sang, J. Lu, S. Lu, Q. Wen, and H. Zhang, Pulse duration dependent nonlinear optical response in black phosphorus dispersions, *Opt. Commun.* 406, 244 (2018)
11. R. Gusmão, Z. Sofer, and M. Pumera, Black phosphorus rediscovered: From bulk material to monolayers, *Angew. Chem. Int. Ed. Engl.* 56(28), 8052 (2017)
12. B. Guo, Q. Xiao, S. Wang, and H. Zhang, 2D layered materials: Synthesis, nonlinear optical properties, and device applications, *Laser Photonics Rev.* 13(12), 1800327 (2019)
13. Y. Xu, X. Jiang, Y. Ge, Z. Guo, Z. Zeng, Q. Xu, H. Zhang, X. Yu, and D. Fan, Size-dependent nonlinear optical properties of black phosphorus nanosheets and their applications in ultrafast photonics, *J. Mater. Chem. C* 5(12), 3007 (2017)
14. P. W. Bridgman, Two new modifications of phosphorus, *J. Am. Chem. Soc.* 36(7), 1344 (1914)
15. E. S. Reich, Phosphorene excites materials scientists, *Nature* 506(7486), 19 (2014)
16. B. Gao, C. Ma, J. Huo, Y. Guo, T. Sun, and G. Wu, Influence of gain fiber on dissipative soliton pairs in passively mode-locked fiber laser based on BP as a saturable absorber, *Opt. Commun.* 410, 191 (2018)
17. Z. Wang, Y. Xu, S. C. Dhanabalan, J. Sophia, C. Zhao, C. Xu, Y. Xiang, J. Li, and H. Zhang, Black phosphorus quantum dots as an efficient saturable absorber for bound soliton operation in an erbium doped fiber laser, *IEEE Photonics J.* 8(5), 1503310 (2016)
18. D. Mao, M. Li, X. Cui, W. Zhang, H. Lu, K. Song, and J. Zhao, Stable high-power saturable absorber based on polymer-black-phosphorus films, *Opt. Commun.* 406, 254 (2018)
19. J. Liu, F. Zhao, H. Wang, W. Zhang, X. Hu, X. Li, and Y. Wang, Generation of dark solitons in erbium-doped fiber laser based on black phosphorus nanoparticles, *Opt. Mater.* 89, 100 (2019)
20. X. Liu, Q. Guo, and J. Qiu, Emerging low-dimensional materials for nonlinear optics and ultrafast photonics, *Adv. Mater.* 29(14), 1605886 (2017)
21. A. Naskar and K. S. Kim, Black phosphorus nanomaterials as multi-potent and emerging platforms against bacterial infections, *Microb. Pathog.* 137, 103800 (2019)
22. Y. Wang, G. Qiu, R. Wang, S. Huang, Q. Wang, Y. Liu, Y. Du, W. III Goddard, M. Kim, X. Xu, P. Ye, and W. Wu, Field-effect transistors made from solution-grown two-dimensional tellurene, *Nat. Electron* 1(4), 228 (2018)
23. S. A. Hussain, Discovery of several new families of saturable absorbers for ultrashort pulsed laser systems, *Sci. Rep.* 9(1), 19910 (2019)
24. T. Hai, G. Xie, Z. Qiao, Z. Qin, J. Ma, Y. Sun, F. Wang, P. Yuan, J. Ma, and L. Qian, Indium selenide film: a promising saturable absorber in 3- to 4-μm band for mid-infrared pulsed laser, *Nanophotonics* 9(7), 2045 (2020)
25. Y. Li, C. Yu, Z. Li, P. Jiang, X. Zhou, C. Gao, and J. Li, Layer-dependent and light-tunable surface potential of two-dimensional indium selenide (InSe) flakes, *Rare Met.* 39(12), 1356 (2020)
26. F. J. Manjón, A. Segura, and V. Muñoz, High density photoluminescence induced by laser pulse excitation in InSe under pressure, *High Press. Res.* 18(1-6), 81 (2000)
27. S. Li, C. Wang, Y. Yin, E. Lewis, and P. Wang, Novel layered 2D materials for ultrafast photonics, *Nanophotonics* 9(7), 1743 (2020)
28. R. Zhou, K. Ullah, S. Yang, Q. Lin, L. Tang, D. Liu, S. Li, Y. Zhao, and F. Wang, Recent advances in graphene and black phosphorus nonlinear plasmonics, *Nanophotonics* 9(7), 1695 (2020)
29. X. Liu, Q. Gao, Y. Zheng, D. Mao, and J. Zhao, Recent progress of pulsed fiber lasers based on transition-metal dichalcogenides and black phosphorus saturable absorbers, *Nanophotonics* 9(8), 2215 (2020)
30. C. Zhang, Y. Chen, T. Fan, Y. Ge, C. Zhao, H. Zhang, and S. Wen, Sub-hundred nanosecond pulse generation from a black phosphorus Q-switched Er-doped fiber laser, *Opt. Express* 28(4), 4708 (2020)
31. D. Wang, H. Song, X. Long, and L. Li, Switchable and tunable multi-wavelength emissions in pulsed ytterbium fiber lasers with black phosphorus saturable absorbers and polarization-maintaining fiber Bragg gratings, *Opt. Commun.* 452, 373 (2019)
32. X. Shi, Z. Tong, W. Zhang, J. Qin, H. Pan, and C. Sun, Tunable multiwavelength erbium-doped fiber laser based on BPQDs packaged by poly tetra fluoroethylene and two segments of PMF, *Opt. Commun.* 453, 124349 (2019)
33. J. Sotor, G. Sobon, W. Macherzynski, P. Paletko, and K. M. Abramski, Black phosphorus saturable absorber for ultrashort pulse generation, *Appl. Phys. Lett.* 107(5), 051108 (2015)
34. M. Zhang, Q. Wu, F. Zhang, L. Chen, X. Jin, Y. Hu, Z. Zheng, and H. Zhang, 2D black phosphorus saturable absorbers for ultrafast photonics, *Adv. Opt. Mater.* 7(1), 1800224 (2019)
35. H. Liu, W. Song, Y. Yu, Q. Jiang, F. Pang, and T. Wang, Black phosphorus-film with drop-casting method for high-energy pulse generation From Q-switched Er-doped fiber laser, *Photonic Sens.* 9(3), 239 (2019)
36. P. Guo, X. Li, T. Chai, T. Feng, Y. Ge, Y. Song, and Y. Wang, Few-layer bismuthene for robust ultrafast photonics in C-band optical communications, *Nanotechnology* 30(35), 354002 (2019)

37. H. Luo, X. Tian, Y. Gao, R. Wei, J. Li, J. Qiu, and Y. Liu, Antimonene: A long-term stable two-dimensional saturable absorption material under ambient conditions for the mid-infrared spectral region, *Photon. Res.* 6(9), 900 (2018)
38. L. Huang and K. W. Ang, Black phosphorus photonics toward on-chip applications, *Phys. Rev. Appl.* 7(3), 031302 (2020)
39. A. H. H. Al-Masoodi, M. Yasin, M. H. M. Ahmed, A. A. Latiff, H. Arof, and S. W. Harun, Mode-locked ytterbium-doped fiber laser using mechanically exfoliated black phosphorus as saturable absorber, *Optik (Stuttg.)* 147, 52 (2017)
40. C. Shang, Y. Zhang, H. Qin, B. He, C. Zhang, J. Sun, J. Li, J. Ma, X. Ji, L. Xu, and B. Fu, Review on wavelength-tunable pulsed fiber lasers based on 2D materials, *Opt. Laser Technol.* 131, 106375 (2020)
41. Y. Zhang, S. Wang, S. Chen, Q. Zhang, X. Wang, X. Zhu, X. Zhang, X. Xu, T. Yang, M. He, X. Yang, Z. Li, X. Chen, M. Wu, Y. Lu, R. Ma, W. Lu, and A. Pan, Wavelength-tunable mid-infrared lasing from black phosphorus nanosheets, *Adv. Mater.* 32(17), e1808319 (2020)
42. Y. Zhang, D. Lu, H. Yu, and H. Zhang, Low-dimensional saturable absorbers in the visible spectral region, *Adv. Opt. Mater.* 7(1), 1800886 (2019)
43. Y. Han, Y. Guo, B. Gao, C. Ma, R. Zhang, and H. Zhang, Generation, optimization, and application of ultrashort femtosecond pulse in mode-locked fiber lasers, *Prog. Quantum Electron.* 71, 100264 (2020)
44. B. Gao, R. H. Zhang, J. Y. Huo, C. Y. Ma, Y. Han, Q. R. Hou, F. Deng, G. Wu, and Y. Q. Ge, Generation and categories of solitons in various mode-locked fiber lasers, *Optik (Stuttg.)* 220, 165168 (2020)
45. Y. Han, B. Gao, Y. Y. Li, J. Y. Huo, and Y. B. Guo, Numerical simulation of two-soliton and three-soliton molecules evolution in passively mode-locked fiber laser, *Optik (Stuttg.)* 223, 165381 (2020)
46. Y. Zhao, P. Guo, X. Li, and Z. Jin, Ultrafast photonics application of graphdiyne in the optical communication region, *Carbon* 149, 336 (2019)
47. H. Song, Q. Wang, Y. Zhang, and L. Li, Mode-locked ytterbium-doped all-fiber lasers based on few-layer black phosphorus saturable absorbers, *Opt. Commun.* 394, 157 (2017)
48. J. Wang, H. Yuan, H. Chen, J. Yin, J. Li, T. He, C. Guo, P. Yan, J. Wang, R. Yang, X. Zeng, and S. Ruan, Ultrafast pulse generation for Er- and Tm-doped fiber lasers with Sb thin film saturable absorber, *J. Lightwave Technol.* 38(14), 3710 (2020)
49. M. Zhang, J. Li, H. Chen, J. Zhang, J. Yin, T. He, J. Wang, M. Zhang, B. Zhang, J. Yuan, P. Yan, and S. Ruan, Group IIIA/IVA monochalcogenides nanosheets for ultrafast photonics, *APL Photonics* 4(9), 090801 (2019)
50. Q. Guo, J. Pan, Y. Liu, H. Si, Z. Lu, X. Han, J. Gao, Z. Zuo, H. Zhang, and S. Jiang, Output energy enhancement in a mode-locked Er-doped fiber laser using CVD-Bi2Se3 as a saturable absorber, *Opt. Express* 27(17), 24670 (2019)
51. E. Kovalska, J. Luxa, T. Hartman, N. Antonatos, P. Shaban, E. Oparin, M. Zhukova, and Z. Sofer, Non-aqueous solution-processed phosphorene by controlled low-potential electrochemical exfoliation and thin film preparation, *Nanoscale* 12(4), 2638 (2020)
52. H. Liu, Z. Li, Y. Yu, J. Lin, S. Liu, F. Pang, and T. Wang, Nonlinear optical properties of anisotropic two-dimensional layered materials for ultrafast photonics, *Nanophotonics* 9(7), 1651 (2020)
53. Y. Chen, G. Jiang, S. Chen, Z. Guo, X. Yu, C. Zhao, H. Zhang, Q. Bao, S. Wen, D. Tang, and D. Fan, Mechanically exfoliated black phosphorus as a new saturable absorber for both Q-switching and mode-locking laser operation, *Opt. Express* 23(10), 12823 (2015)
54. G. Tiouitchi, M. A. Ali, A. Benyoussef, M. Hamedoun, A. Lachgar, M. Benaissa, A. Kara, A. Ennaoui, A. Mahmoud, F. Boschini, H. Oughaddou, A. El Kenz, and O. Mounkachi, An easy route to synthesize high-quality black phosphorus from amorphous red phosphorus, *Mater. Lett.* 236, 56 (2019)
55. J. R. Brent, N. Savjani, E. A. Lewis, S. J. Haigh, D. J. Lewis, and P. O'Brien, Production of few-layer phosphorene by liquid exfoliation of black phosphorus, *Chem. Commun. (Camb.)* 50(87), 13338 (2014)
56. A. Ambrosi, and M. Pumera, Exfoliation of layered materials using electrochemistry, *Chem. Soc. Rev.* 47(19), 7213 (2018)
57. S. Yang, A. Kim, J. Park, H. Kwon, P. T. Lanh, S. Hong, K. J. Kim, and J. W. Kim, Thermal annealing of black phosphorus for etching and protection, *Appl. Surf. Sci.* 457, 773 (2018)
58. J. Jia, S. K. Jang, S. Lai, J. Xu, Y. J. Choi, J. H. Park, and S. Lee, Plasma-treated thickness-controlled two-dimensional black phosphorus and its electronic transport properties, *ACS Nano* 9(9), 8729 (2015)
59. Z. J. Han, A. T. Murdock, D. H. Seo, and A. Bendavid, Recent progress in plasma-assisted synthesis and modification of 2D materials, *2D Mater.* 5(3), 032002 (2018)
60. B. Guo, S. H. Wang, Z. X. Wu, Z. X. Wang, D. H. Wang, H. Huang, F. Zhang, Y. Q. Ge, and H. Zhang, Sub-200 fs soliton mode-locked fiber laser based on bismuthene saturable absorber, *Opt. Express* 26(18), 22750 (2018)
61. L. Lu, Z. Liang, L. Wu, Y. Chen, Y. Song, S. C. Dhanabalan, J. S. Ponraj, B. Dong, Y. Xiang, F. Xing, D. Fan, and H. Zhang, Few-layer bismuthene: Sonochemical exfoliation, nonlinear optics and applications for ultrafast photonics with enhanced stability, *Laser Photonics Rev.* 12(1), 1700221 (2018)
62. C. Wang, L. Wang, X. Li, W. Luo, T. Feng, Y. Zhang, P. Guo, and Y. Ge, Few-layer bismuthene for femtosecond soliton molecules generation in Er-doped fiber laser, *Nanotechnology* 30(2), 025204 (2019)
63. T. Chai, X. Li, T. Feng, P. Guo, Y. Song, Y. Chen, and H. Zhang, Few-layer bismuthene for ultrashort pulse generation in a dissipative system based on an evanescent field, *Nanoscale* 10(37), 17617 (2018)
64. J. Zhu, X. Liu, M. Xue, and C. Chen, Phosphorene: Synthesis, structure, properties and device applications, *Acta Phys. -Chim. Sin.* 33(11), 2153 (2017)

65. Z. Hui, M. Qu, X. Li, Y. Guo, J. Li, L. Jing, and Z. Wu, SnS nanosheets for harmonic pulses generation in near infrared region, *Nanotechnology* 31(48), 485706 (2020)

66. J. Feng, X. Li, A. Qyyum, Y. Zhang, C. Zheng, Y. Wang, J. Liu, J. Lu, and G. Zhu, SnS nanosheets for 105th harmonic soliton molecule generation, *Ann. Phys-Berlin* 531(10), 1900273 (2019)

67. H. Zhu, D. Yang, Y. Ji, H. Zhang, and X. Shen, Two-dimensional SnS nanosheets fabricated by a novel hydrothermal method, *J. Mater. Sci.* 40(3), 591 (2005)

68. X. Wang, J. Song, and J. Qu, Antimonene: From experimental preparation to practical application, *Angew. Chem. Int. Ed. Engl.* 58(6), 1574 (2019)

69. F. Yang, Y. Liang, L. X. Liu, Q. Zhu, W. H. Wang, X. T. Zhu, and J. D. Guo, Controlled growth of complex polar oxide films with atomically precise molecular beam epitaxy, *Front. Phys.* 13(5), 136802 (2018)

70. H. Yuan, F. Zhu, J. Wang, R. Yang, N. Wang, Y. Yu, P. Yan, and J. Guo, Generation of ultra-fast pulse based on bismuth saturable absorber, *Wuli Xuebao* 69(9), 094203 (2020)

71. K. S. Novoselov, A. K. Geim, S. V. Morozov, D. Jiang, M. I. Katsnelson, I. V. Grigorieva, S. V. Dubonos, and A. A. Firsov, Two-dimensional gas of massless Dirac fermions in graphene, *Nature* 438(7065), 197 (2005)

72. S. Wu, K. S. Hui, and K. N. Hui, 2D black phosphorus: From preparation to applications for electrochemical energy storage, *Adv. Sci. (Weinh.)* 5(5), 1700491 (2018)

73. J. Wang, X. Wang, J. Lei, M. Ma, C. Wang, Y. Ge, and Z. Wei, Recent advances in mode-locked fiber lasers based on two-dimensional materials, *Nanophotonics* 9(8), 2315 (2020)

74. C. Ma, C. Wang, B. Gao, J. Adams, G. Wu, and H. Zhang, Recent progress in ultrafast lasers based on 2D materials as a saturable absorber, *Phys. Rev. Appl.* 6(4), 041304 (2019)

75. N. Li, Q. Wang, and H.L. Zhang, 2D materials in light: Excited-state dynamics and applications, *Chem. Rec.* 20(5), 413 (2020)

76. H. Ahmad, S. A. Reduan, S. I. Ooi, and M. A. Ismail, Mechanically exfoliated In2Se3 as a saturable absorber for mode-locking a thulium-doped fluoride fiber laser operating in S-band, *Appl. Opt.* 57(24), 6937 (2018)

77. Z. Qin, G. Xie, H. Zhang, C. Zhao, P. Yuan, S. Wen, and L. Qian, Black phosphorus as saturable absorber for the Q-switched Er:ZBLAN fiber laser at 2.8 μm, *Opt. Express* 23(19), 24713 (2015)

78. S. Su, B. Xu, J. Ding, and H. Yu, Large-yield exfoliation of few-layer black phosphorus nanosheets in liquid, *New J. Chem.* 43(48), 19365 (2019)

79. Z. Guo, H. Zhang, S. Lu, Z. Wang, S. Tang, J. Shao, Z. Sun, H. Xie, H. Wang, X. F. Yu, and P. K. Chu, From black phosphorus to phosphorene: Basic solvent exfoliation, evolution of Raman scattering, and applications to ultrafast photonics, *Adv. Funct. Mater.* 25(45), 6996 (2015)

80. Y. Song, Z. Liang, X. Jiang, Y. Chen, Z. Li, L. Lu, Y. Ge, K. Wang, J. Zheng, S. Lu, J. Ji, and H. Zhang, Few-layer antimonene decorated microfiber: ultra-short pulse generation and all-optical thresholding with enhanced long term stability, *2D Mater.* 4(4), 045010 (2017)

81. C. Xing, J. Zhang, J. Jing, J. Li, and F. Shi, Preparations, properties and applications of low-dimensional black phosphorus, *Chem. Eng. J.* 370, 120 (2019)

82. W. Zhang, G. Wang, F. Xing, Z. Man, F. Zhang, K. Han, H. Zhang, and S. Fu, Passively Q-switched and mode-locked erbium-doped fiber lasers based on tellurene nanosheets as saturable absorber, *Opt. Express* 28(10), 14729 (2020)

83. W. Yang, N. Xu, and H. Zhang, Nonlinear absorption properties of indium selenide and its application for demonstrating pulsed Er-doped fiber laser, *Laser Phys. Lett.* 15(10), 105101 (2018)

84. N. Xu, W. Yang, and H. Zhang, Nonlinear saturable absorption properties of indium selenide and its application for demonstrating a Yb-doped mode-locked fiber laser, *Opt. Mater. Express* 8(10), 3092 (2018)

85. Z. Xie, C. Xing, W. Huang, T. Fan, Z. Li, J. Zhao, Y. Xiang, Z. Guo, J. Li, Z. Yang, B. Dong, J. Qu, D. Fan, and H. Zhang, Ultrathin 2D Nonlayered Tellurium Nanosheets: Facile Liquid-Phase Exfoliation, Characterization, and Photoresponse with High Performance and Enhanced Stability, *Adv. Funct. Mater.* 28(16), 1705833 (2018)

86. B. Fu, J. Sun, G. Wang, C. Shang, Y. Ma, J. Ma, L. Xu, and V. Scardaci, Solution-processed two-dimensional materials for ultrafast fiber lasers (invited), *Nanophotonics* 9(8), 2169 (2020)

87. J. B. Smith, D. Hagaman, and H. F. Ji, Growth of 2D black phosphorus film from chemical vapor deposition, *Nanotechnology* 27(21), 215602 (2016)

88. W. Liu, Y. Zhu, X. Xu, S. Wang, and X. Zhang, Preparation of few-layer black phosphorus by wet ball milling exfoliation, *J. Mater. Sci. Mater. Electron.* 31(12), 9543 (2020)

89. Q. Q. Yang, R. T. Liu, C. Huang, Y. F. Huang, L. F. Gao, B. Sun, Z. P. Huang, L. Zhang, C. X. Hu, Z. Q. Zhang, C. L. Sun, Q. Wang, Y. L. Tang, and H.L. Zhang, 2D bismuthene fabricated *via* acid-intercalated exfoliation showing strong nonlinear near-infrared responses for mode-locking lasers, *Nanoscale* 10(45), 21106 (2018)

90. J. Pei, X. Gai, J. Yang, X. Wang, Z. Yu, D. Y. Choi, B. Luther-Davies, and Y. Lu, Producing air-stable monolayers of phosphorene and their defect engineering, *Nat. Commun.* 7(1), 10450 (2016)

91. V. Eswaraiah, Q. Zeng, Y. Long, and Z. Liu, Black phosphorus nanosheets: Synthesis, characterization and applications, *Small* 12(26), 3480 (2016)

92. J. Y. Xu, L. F. Gao, C. X. Hu, Z. Y. Zhu, M. Zhao, Q. Wang, and H. L. Zhang, Preparation of large size, few-layer black phosphorus nanosheets via phytic acid-assisted liquid exfoliation, *Chem. Commun. (Camb.)* 52(52), 8107 (2016)

93. H. Xiao, M. Zhao, J. Zhang, X. Ma, J. Zhang, T. Hu, T. Tang, J. Jia, and H. Wu, Electrochemical cathode exfoliation of bulky black phosphorus into few-layer phosphorene nanosheets, *Electrochem. Commun.* 89, 10 (2018)
94. S. Yang, K. Zhang, A. G. Ricciardulli, P. Zhang, Z. Liao, M. R. Lohe, E. Zschech, P. W. M. Blom, W. Pisula, K. Mullen, and X. Feng, A delamination strategy for thinly layered defect-free high-mobility black phosphorus flakes, *Angew. Chem. Int. Ed. Engl.* 57(17), 4677 (2018)
95. Q. Hao, J. Liu, G. Wang, J. Chen, H. Gan, J. Zhu, Y. Ke, Y. Chai, J. Lin, and W. Zhang, Surface-modified ultrathin inse nanosheets with enhanced stability and photoluminescence for high-performance optoelectronics, *ACS Nano* 14(9), 11373 (2020)
96. Z. Yang, J. Hao, S. Yuan, S. Lin, H. M. Yau, J. Dai, and S. P. Lau, Field-effect transistors based on amorphous black phosphorus ultrathin films by pulsed laser deposition, *Adv. Mater.* 27(25), 3748 (2015)
97. J. Ji, X. Song, J. Liu, Z. Yan, C. Huo, S. Zhang, M. Su, L. Liao, W. Wang, Z. Ni, Y. Hao, and H. Zeng, Two-dimensional antimonene single crystals grown by van der Waals epitaxy, *Nat. Commun.* 7(1), 13352 (2016)
98. Q. Sun, X. Zhao, Y. Feng, Y. Wu, Z. Zhang, X. Zhang, X. Wang, S. Feng, and X. Liu, Pressure quenching: a new route for the synthesis of black phosphorus, *Inorg. Chem. Front.* 5(3), 669 (2018)
99. K. Wang, X. Zhang, I. M. Kislyakov, N. Dong, S. Zhang, G. Wang, J. Fan, X. Zou, J. Du, Y. Leng, Q. Zhao, K. Wu, J. Chen, S. M. Baesman, K. S. Liao, S. Maharjan, H. Zhang, L. Zhang, S. A. Curran, R. S. Oremland, W. J. Blau, and J. Wang, Bacterially synthesized tellurium nanostructures for broadband ultrafast nonlinear optical applications, *Nat. Commun.* 10(1), 3985 (2019)
100. B. Wang, S. Zhong, Y. Ge, H. Wang, X. Luo, and H. Zhang, Present advances and perspectives of broadband photo-detectors based on emerging 2D-Xenes beyond graphene, *Nano Res.* 13(4), 891 (2020)
101. H. Liu, Y. Du, Y. Deng, and P. D. Ye, Semiconducting black phosphorus: Synthesis, transport properties and electronic applications, *Chem. Soc. Rev.* 44(9), 2732 (2015)
102. A. Castellanos-Gomez, Black phosphorus: Narrow gap, wide applications, *J. Phys. Chem. Lett.* 6(21), 4280 (2015)
103. X. Wang and S. Lan, Optical properties of black phosphorus, *Adv. Opt. Photonics* 8(4), 618 (2016)
104. X. Ling, H. Wang, S. Huang, F. Xia, and M. S. Dresselhaus, The renaissance of black phosphorus, *Proc. Natl. Acad. Sci. U.S.A.* 112(15), 4523 (2015)
105. X. Chen, J. S. Ponraj, D. Fan, and H. Zhang, An overview of the optical properties and applications of black phosphorus, *Nanoscale* 12(6), 3513 (2020)
106. D. Zhang, Z. Yuan, G. Zhang, N. Tian, D. Liu, and Y. Zhang, Preparation and characterization of black phosphorus, *Acta Chimi. Sin.* 76(7), 537 (2018)
107. S. Zhang, X. Zhang, H. Wang, B. Chen, K. Wu, K. Wang, D. Hanlon, J. N. Coleman, J. Chen, L. Zhang, and J. Wang, Size-dependent saturable absorption and mode-locking of dispersed black phosphorus nanosheets, *Opt. Mater. Express* 6(10), 3159 (2016)
108. K. S. Novoselov, D. V. Andreeva, W. Ren, and G. Shan, Graphene and other two-dimensional materials, *Front. Phys.* 14(1), 13301 (2019)
109. J. C. Lei, X. Zhang, and Z. Zhou, Recent advances in MXene: Preparation, properties, and applications, *Front. Phys.* 10(3), 276 (2015)
110. F. Xia, H. Wang, and Y. Jia, Rediscovering black phosphorus as an anisotropic layered material for optoelectronics and electronics, *Nat. Commun.* 5(1), 4458 (2014)
111. J. Zou, Q. Ruan, X. Zhang, B. Xu, Z. Cai, and Z. Luo, Visible-wavelength pulsed lasers with low-dimensional saturable absorbers, *Nanophotonics* 9(8), 2273 (2020)
112. T. Wang, W. Zhang, X. Shi, J. Wang, X. Ding, K. Zhang, J. Peng, J. Wu, and P. Zhou, Black phosphorus-enabled harmonic mode locking of dark pulses in a Yb-doped fiber laser, *Laser Phys. Lett.* 16(8), 085102 (2019)
113. L. Xian, A. Pérez Paz, E. Bianco, P. M. Ajayan and A. Rubio, Square selenene and tellurene: Novel group VI elemental 2D materials with nontrivial topological properties, *2D Mater.* 4(4), 041003 (2017)
114. Z. Zhu, X. Cai, S. Yi, J. Chen, Y. Dai, C. Niu, Z. Guo, M. Xie, F. Liu, J. H. Cho, Y. Jia, and Z. Zhang, Multivalency-driven formation of Te-based monolayer materials: A combined first-principles and experimental study, *Phys. Rev. Lett.* 119(10), 106101 (2017)
115. J. Guo, J. Zhao, D. Huang, Y. Wang, F. Zhang, Y. Ge, Y. Song, C. Xing, D. Fan, and H. Zhang, Two-dimensional tellurium-polymer membrane for ultrafast photonics, *Nanoscale* 11(13), 6235 (2019)
116. F. Zhang, G. Liu, Z. Wang, T. Tang, X. Wang, C. Wang, S. Fu, F. Xing, K. Han, and X. Xu, Broadband nonlinear absorption properties of two-dimensional hexagonal tellurene nanosheets, *Nanoscale* 11(36), 17058 (2019)
117. Z. Shi, R. Cao, K. Khan, A. K. Tareen, X. Liu, W. Liang, Y. Zhang, C. Ma, Z. Guo, X. Luo, and H. Zhang, Two-dimensional tellurium: Progress, challenges, and prospects, *Nano-Micro Lett.* 12(1), 99 (2020)
118. N. Xu, P. Ma, S. Fu, X. Shang, S. Jiang, S. Wang, D. Li, and H. Zhang, Tellurene-based saturable absorber to demonstrate large-energy dissipative soliton and noise-like pulse generations, *Nanophotonics* 9(9), 2783 (2020)
119. S. Zhang, S. Guo, Z. Chen, Y. Wang, H. Gao, J. Gomez-Herrero, P. Ares, F. Zamora, Z. Zhu, and H. Zeng, Recent progress in 2D group-VA semiconductors: From theory to experiment, *Chem. Soc. Rev.* 47(3), 982 (2018)
120. G. Wang, R. Pandey, and S. P. Karna, Atomically thin group V elemental films: Theoretical investigations of antimonene allotropes, *ACS Appl. Mater. Interfaces* 7(21), 11490 (2015)
121. P. Hu, Y. Liu, L. Guo, X. Ge, X. Liu, L. Yu, and Q. Liu, Passively Q-switched erbium-doped fiber laser based on antimonene as saturable absorber, *Appl. Opt.* 58(28), 7845 (2019)
122. G. Liu, F. Zhang, T. Wu, Z. Li, W. Zhang, K. Han, F. Xing, Z. Man, X. Ge, and S. Fu, Single- and dual-wavelength passively mode-locked erbium-doped fiber laser based on antimonene saturable absorber, *IEEE Photonics J.* 11(3), 1 (2019)

123. T. Feng, X. Li, T. Chai, P. Guo, Y. Zhang, R. Liu, J. Liu, J. Lu, and Y. Ge, Bismuthene nanosheets for 1 μm multipulse generation, *Langmuir* 36(1), 3 (2020)

124. J. He, L. Tao, H. Zhang, B. Zhou, and J. Li, Emerging 2D materials beyond graphene for ultrashort pulse generation in fiber lasers, *Nanoscale* 11(6), 2577 (2019)

125. Z. Yang, Z. Wu, Y. Lyu, and J. Hao, Centimeter-scale growth of two-dimensional layered high-mobility bismuth films by pulsed laser deposition, *InfoMat* 1(1), 98 (2019)

126. D. A. Bandurin, A. V. Tyurnina, G. L. Yu, A. Mishchenko, V. Zolyomi, S. V. Morozov, R. K. Kumar, R. V. Gorbachev, Z. R. Kudrynskyi, S. Pezzini, Z. D. Kovalyuk, U. Zeitler, K. S. Novoselov, A. Patane, L. Eaves, I. V. Grigorieva, V. I. Fal'ko, A. K. Geim, and Y. Cao, High electron mobility, quantum Hall effect and anomalous optical response in atomically thin InSe, *Nat. Nanotechnol.* 12(3), 223 (2017)

127. J. Quereda, R. Biele, G. Rubio-Bollinger, N. Agraït, R. D'Agosta, and A. Castellanos-Gomez, Strong quantum confinement effect in the optical properties of ultrathin α-In_2Se_3, *Adv. Opt. Mater.* 4(12), 1939 (2016)

128. M. Yüksek, H. G. Yaglioglu, A. Elmali, E. M. Aydın, U. Kürüm, and A. Ateş, Nonlinear and saturable absorption characteristics of Ho doped InSe crystals, *Opt. Commun.* 310, 100 (2014)

129. H. Long, S. Liu, Q. Wen, H. Yuan, C. Y. Tang, J. Qu, S. Ma, W. Qarony, L. H. Zeng, and Y. H. Tsang, In_2Se_3 nanosheets with broadband saturable absorption used for near-infrared femtosecond laser mode locking, *Nanotechnology* 30(46), 465704 (2019)

130. X. Han, H. Zhang, S. Jiang, C. Zhang, D. Li, Q. Guo, J. Gao, and B. Man, Improved laser damage threshold of In2Se3 saturable absorber by PVD for high-power mode-locked Er-doped fiber laser, *Nanomaterials (Basel)* 9(9), 1216 (2019)

131. H. Tian, J. Tice, R. Fei, V. Tran, X. Yan, L. Yang, and H. Wang, Low-symmetry two-dimensional materials for electronic and photonic applications, *Nano Today* 11(6), 763 (2016)

132. L. Liu, L. Yu, X. L. Li, Z. B. Wang, and Q. Liang, Structure and optical properties of Cu-doped SnS thin films prepared by PLD, *Chin. J. Lumin.* 36(11), 1311 (2015)

133. Z. Xie, F. Zhang, Z. Liang, T. Fan, Z. Li, X. Jiang, H. Chen, J. Li, and H. Zhang, Revealing of the ultrafast third-order nonlinear optical response and enabled photonic application in two-dimensional tin sulfide, *Photon. Res.* 7(5), 494 (2019)

134. Y. Li, Y. He, Y. Cai, S. Chen, J. Liu, Y. Chen, and X. Yuanjiang, Black phosphorus: Broadband nonlinear optical absorption and application, *Laser Phys. Lett.* 15(2), 025301 (2018)

135. T. Wang, W. Zhang, J. Wang, J. Wu, T. Hou, P. Ma, R. Su, Y. Ma, J. Peng, L. Zhan, K. Zhang, and P. Zhou, Bright/dark switchable mode-locked fiber laser based on black phosphorus, *Opt. Laser Technol.* 123, 105948 (2020)

136. M. B. Hisyam, M. F. M. Rusdi, A. A. Latiff, and S. W. Harun, Generation of mode-locked ytterbium doped fiber ring laser using few-layer black phosphorus as a saturable absorber, *IEEE J. Sel. Top. Quant.* 23(1), 39 (2017)

137. X. Jin, G. Hu, M. Zhang, Y. Hu, T. Albrow-Owen, R. C. T. Howe, T. C. Wu, Q. Wu, Z. Zheng, and T. Hasan, 102 fs pulse generation from a long-term stable, inkjet-printed black phosphorus-mode-locked fiber laser, *Opt. Express* 26(10), 12506 (2018)

138. H. Yu, X. Zheng, K. Yin, X. Cheng, and T. Jiang, Thulium/holmium-doped fiber laser passively mode locked by black phosphorus nanoplatelets-based saturable absorber, *Appl. Opt.* 54(34), 10290 (2015)

139. Z. Qin, G. Xie, C. Zhao, S. Wen, P. Yuan, and L. Qian, Mid-infrared mode-locked pulse generation with multilayer black phosphorus as saturable absorber, *Opt. Lett.* 41(1), 56 (2016)

140. Q. Feng, H. Liu, M. Zhu, J. Shang, D. Liu, X. Cui, D. Shen, L. Kou, D. Mao, J. Zheng, C. Li, J. Zhang, H. Xu, and J. Zhao, Electrostatic functionalization and passivation of water-exfoliated few-layer black phosphorus by poly dimethyldiallyl ammonium chloride and its ultrafast laser application, *ACS Appl. Mater. Interfaces* 10(11), 9679 (2018)

141. K. Park, J. Lee, Y. T. Lee, W. K. Choi, J. H. Lee, and Y. W. Song, Black phosphorus saturable absorber for ultrafast mode-locked pulse laser via evanescent field interaction, *Ann. Phys-Berlin* 527(11–12), 770 (2015)

142. D. Li, H. Jussila, L. Karvonen, G. Ye, H. Lipsanen, X. Chen, and Z. Sun, Polarization and thickness dependent absorption properties of black phosphorus: New saturable absorber for ultrafast pulse generation, *Sci. Rep.* 5(1), 15899 (2015)

143. L. Yun, Black phosphorus saturable absorber for dual-wavelength polarization-locked vector soliton generation, *Opt. Express* 25(26), 32380 (2017)

144. Y. Song, S. Chen, Q. Zhang, L. Li, L. Zhao, H. Zhang, and D. Tang, Vector soliton fiber laser passively mode locked by few layer black phosphorus-based optical saturable absorber, *Opt. Express* 24(23), 25933 (2016)

145. M. H. M. Ahmed, A. A. Latiff, H. Arof, and S. W. Harun, Ultrafast erbium-doped fiber laser mode-locked with a black phosphorus saturable absorber, *Laser Phys. Lett.* 13(9), 095104 (2016)

146. C. Gao, S. Lv, G. Zhu, G. Wang, X. Su, B. Wang, S. Kumar, R. Dou, F. Peng, Q. Zhang, H. Yu, X. Lin, and B. Zhang, Self-Q-switching and passively Q-switched mode-locking of dual-wavelength Nd:YSAG laser, *Opt. Laser Technol.* 122, 105860 (2020)

147. L. Li, Y. Wang, and X. Wang, Ultrafast pulse generation with black phosphorus solution saturable absorber, *Laser Phys.* 27(8), 085104 (2017)

148. E. I. Ismail, N. A. Kadir, A. A. Latiff, H. Ahmad, and S. W. Harun, Black phosphorus crystal as a saturable absorber for both a Q-switched and mode-locked erbium-doped fiber laser, *RSC Adv.* 6(76), 72692 (2016)

149. D. Na, K. Park, K. H. Park, and Y. W. Song, Passivation of black phosphorus saturable absorbers for reliable pulse formation of fiber lasers, *Nanotechnology* 28(47), 475207 (2017)

150. Z. C. Luo, M. Liu, Z. N. Guo, X. F. Jiang, A. P. Luo, C. J. Zhao, X. F. Yu, W. C. Xu, and H. Zhang, Microfiber-based few-layer black phosphorus saturable absorber for ultra-fast fiber laser, *Opt. Express* 23(15), 20030 (2015)

151. Y. Chen, S. Chen, J. Liu, Y. Gao, and W. Zhang, Sub-300 femtosecond soliton tunable fiber laser with all-anomalous dispersion passively mode locked by black phosphorus, *Opt. Express* 24(12), 13316 (2016)

152. W. Li, G. Chen, G. Wang, C. Zeng, and W. Zhao, Wide-band wavelength-tunable ultrafast fiber laser based on black phosphorus saturable absorber, *Laser Phys. Lett.* 15(12), 125102 (2018)

153. J. Du, M. Zhang, Z. Guo, J. Chen, X. Zhu, G. Hu, P. Peng, Z. Zheng, and H. Zhang, Phosphorene quantum dot saturable absorbers for ultrafast fiber lasers, *Sci. Rep.* 7(1), 42357 (2017)

154. M. Liu, X. F. Jiang, Y. R. Yan, X. D. Wang, A. P. Luo, W. C. Xu, and Z. C. Luo, Black phosphorus quantum dots for femtosecond laser photonics, *Opt. Commun.* 406, 85 (2018)

155. Y. Xu, Z. Wang, Z. Guo, H. Huang, Q. Xiao, H. Zhang, and X. F. Yu, Solvothermal synthesis and ultrafast photonics of black phosphorus quantum dots, *Adv. Opt. Mater.* 4(8), 1223 (2016)

156. G. Liu, J. Yuan, T. Wu, F. Zhang, F. Xing, W. Zhang, H. Zhang, and S. Fu, Ultrathin 2D nonlayered tellurene nanosheets as saturable absorber for picosecond pulse generation in all-fiber lasers, *IEEE J. Sel. Top. Quant.* 27(2), 1 (2021)

157. L. Du, D. Lu, J. Li, L. Yang, K. Yang, B. Huang, L. Miao, X. Qi, C. Zhao, J. Zhong, and S. Wen, Antimony thin film as a robust broadband saturable absorber, *IEEE J. Sel. Top. Quant.* 27(2), 1 (2021)

158. W. Xu, P. Guo, X. Li, Z. Hui, Y. Wang, Z. Shi, and Y. Shu, Sheet-structured bismuthene for near-infrared dual-wavelength harmonic mode-locking, *Nanotechnology* 31(22), 225209 (2020)

159. P. Guo, X. Li, T. Feng, Y. Zhang, and W. Xu, Few-layer bismuthene for coexistence of harmonic and dual wavelength in a mode-locked fiber laser, *ACS Appl. Mater. Interfaces* 12(28), 31757 (2020)

160. P. Yan, Z. Jiang, H. Chen, J. Yin, J. Lai, J. Wang, T. He, and J. Yang, α-In_2Se_3 wideband optical modulator for pulsed fiber lasers, *Opt. Lett.* 43(18), 4417 (2018)

161. J. Sotor, G. Sobon, M. Kowalczyk, W. Macherzynski, P. Paletko, and K. M. Abramski, Ultrafast thulium-doped fiber laser mode locked with black phosphorus, *Opt. Lett.* 40(16), 3885 (2015)

162. J. Liu, K. Xia, W. Zhang, J. Zhu, B. Yan, P. Yang, S. Dai, and Q. Nie, Tm-doped all-fiber structured femtosecond laser mode-locked by a novel Chem-Te saturable absorber, *Infrared Phys. Technol.* 108, 103343 (2020)

163. J. Li, H. Luo, B. Zhai, R. Lu, Z. Guo, H. Zhang, and Y. Liu, Black phosphorus: A two-dimension saturable absorption material for mid-infrared Q-switched and mode-locked fiber lasers, *Sci. Rep.* 6(1), 30361 (2016)

164. Z. Qin, T. Hai, G. Xie, J. Ma, P. Yuan, L. Qian, L. Li, L. Zhao, and D. Shen, Black phosphorus Q-switched and mode-locked mid-infrared Er:ZBLAN fiber laser at 3.5 μm wavelength, *Opt. Express* 26(7), 8224 (2018)

165. W. Jia, J. Yu, L. Chai, and C. Y. Wang, Micromachining soda-lime glass by femtosecond laser pulses, *Front. Phys.* 10(4), 1 (2015)

166. Z. Dong, S. Li, R. Chen, H. Li, C. Gu, P. Yao, and L. Xu, Mode-locked ytterbium-doped fiber laser based on offset-spliced graded index multimode fibers, *Opt. Laser Technol.* 119, 105576 (2019)

167. L. Zheng, K. Hu, F. Teng, and X. Fang, Novel UV-visible photodetector in photovoltaic mode with fast response and ultrahigh photosensitivity employing Se/TiO_2 nanotubes heterojunction, *Small* 13(5), 1602448 (2017)

168. J. Li, Y. Ding, D. Wei Zhang, and P. Zhou, Photodetectors based on two-dimensional materials and their van der waals heterostructures, *Acta Phys.-Chem. Sin.* 35(10), 1058 (2019)

169. J. Wu, G. Koon, D. Xiang, C. Han, C. Toh, E. Kulkarni, I. Verzhbitskiy, A. Carvalho, A. Rodin, S. Koenig, G. Eda, W. Chen, A. Neto, and B. Ozyilmaz, Colossal ultraviolet photoresponsivity of few-layer black phosphorus, *ACS Nano* 9(8), 8070 (2015)

170. M. Long, P. Wang, H. Fang, and W. Hu, Progress, challenges, and opportunities for 2D material based photodetectors, *Adv. Funct. Mater.* 29(19), 1803807 (2018)

171. L. Britnell, R. M. Ribeiro, A. Eckmann, R. Jalil, B. D. Belle, A. Mishchenko, Y. J. Kim, R. V. Gorbachev, T. Georgiou, S. V. Morozov, A. N. Grigorenko, A. K. Geim, C. Casiraghi, A. H. C. Neto, and K. S. Novoselov, Strong light-matter interactions in heterostructures of atomically thin films, *Science* 340(6138), 1311 (2013)

172. S. Lan, S. Rodrigues, L. Kang, and W. Cai, Visualizing optical phase anisotropy in black phosphorus, *ACS Photonics* 3(7), 1176 (2016)

173. J. Miao, L. Zhang, and C. Wang, Black phosphorus electronic and optoelectronic devices, *2D Mater.* 6(3), 032003 (2019)

174. M. Buscema, D. J. Groenendijk, S. I. Blanter, G. A. Steele, H. S. van der Zant, and A. Castellanos-Gomez, Fast and broadband photoresponse of few-layer black phosphorus field-effect transistors, *Nano Lett.* 14(6), 3347 (2014)

175. Y. Liu, B. N. Shivananju, Y. Wang, Y. Zhang, W. Yu, S. Xiao, T. Sun, W. Ma, H. Mu, S. Lin, H. Zhang, Y. Lu, C. W. Qiu, S. Li, and Q. Bao, Highly efficient and air-stable infrared photodetector based on 2D layered graphene-black phosphorus heterostructure, *ACS Appl. Mater. Interfaces* 9(41), 36137 (2017)

176. W. Huang, Y. Zhang, Q. You, P. Huang, Y. Wang, Z. N. Huang, Y. Ge, L. Wu, Z. Dong, X. Dai, Y. Xiang, J. Li, X. Zhang, and H. Zhang, Enhanced photodetection properties of tellurium@selenium roll-to-roll nanotube heterojunctions, *Small* 15(23), e1900902 (2019)

177. M. Amani, C. Tan, G. Zhang, C. Zhao, J. Bullock, X. Song, H. Kim, V. R. Shrestha, Y. Gao, K. B. Crozier, M. Scott, and A. Javey, Solution-synthesized high-mobility tellurium nanoflakes for short-wave infrared photodetectors, *ACS Nano* 12(7), 7253 (2018)

178. S. Fu, J. Li, S. Zhang, Z. Bai, T. Wu, and Z. Man, Large-energy mode-locked Er-doped fiber laser based on indium selenide as a modulator, *Opt. Mater. Express* 9(6), 2662 (2019)

179. B. Deng, R. Frisenda, C. Li, X. Chen, A. Castellanos-Gomez, and F. Xia, Progress on black phosphorus photonics, *Adv. Opt. Mater.* 6(19), 1800365 (2018)

180. Y. Wang, F. Zhang, X. Tang, X. Chen, Y. Chen, W. Huang, Z. Liang, L. Wu, Y. Ge, Y. Song, J. Liu, D. Zhang, J. Li, and H. Zhang, All-optical phosphorene phase modulator with enhanced stability under ambient conditions, *Laser Photon. Rev.* 12(6), 1800016 (2018)

181. C. Lin, R. Grassi, T. Low, and A. S. Helmy, Multilayer black phosphorus as a versatile mid-infrared electro-optic material, *Nano Lett.* 16(3), 1683 (2016)

182. M. Xie, S. Zhang, B. Cai, Y. Huang, Y. Zou, B. Guo, Y. Gu, and H. Zeng, A promising two-dimensional solar cell donor: Black arsenic–phosphorus monolayer with 1.54 eV direct bandgap and mobility exceeding 14,000 $cm^2 \cdot V^{-1} \cdot s^{-1}$, *Nano Energy* 28, 433 (2016)

183. X. H. Yu, K. X. Du, and P. Z. Yang, Preparation of low-dimensional black phosphorus and its application in solar cell, *Laser & Optoelectronics Progress* 56(14), 14001 (2019)

184. W. Cheng, N. Singh, W. Elliott, J. Lee, A. Rassoolkhani, X. Jin, E. W. McFarland, and S. Mubeen, Earth-abundant tin sulfide-based photocathodes for solar hydrogen production, *Adv. Sci. (Weinh.)* 5(1), 1700362 (2018)

185. M. Batmunkh, M. Bat-Erdene, and J. G. Shapter, Black phosphorus: Synthesis and application for solar cells, *Adv. Energy Mater.* 8(5), 1701832 (2018)

186. A. G. Ricciardulli and P. W. M. Blom, Solution-processable 2D materials applied in light-emitting diodes and solar cells, *Adv. Mater. Technol.* 5(8), 1900972 (2020)

187. Y. Yang, J. Gao, Z. Zhang, S. Xiao, H. H. Xie, Z. B. Sun, J. H. Wang, C. H. Zhou, Y. W. Wang, X. Y. Guo, P. K. Chu, and X. F. Yu, Black phosphorus based photocathodes in wideband bifacial dye-sensitized solar cells, *Adv. Mater.* 28(40), 8937 (2016)

188. J. Song, J. Wang, X. Lin, J. He, H. Liu, Y. Lei, and Z. Chu, Black phosphorus/TiO2 composite photoanode with enhanced photoelectrical performance, *ChemElectroChem* 4(9), 2373 (2017)

189. L. Li, L. Chen, S. Mukherjee, J. Gao, H. Sun, Z. Liu, X. Ma, T. Gupta, C. V. Singh, W. Ren, H. M. Cheng, and N. Koratkar, Phosphorene as a polysulfide immobilizer and catalyst in high-performance lithium-sulfur batteries, *Adv. Mater.* 29(2), 1602734 (2017)

190. W. Tao, X. Zhu, X. Yu, X. Zeng, Q. Xiao, X. Zhang, X. Ji, X. Wang, J. Shi, H. Zhang, and L. Mei, Black phosphorus nanosheets as a robust delivery platform for cancer theranostics, *Adv. Mater.* 29(1), 1603276 (2017)

191. J. Ouyang, R. Y. Liu, W. Chen, Z. Liu, Q. Xu, K. Zeng, L. Deng, L. Shen, and Y. N. Liu, A black phosphorus based synergistic antibacterial platform against drug resistant bacteria, *J. Mater. Chem. B* 6(39), 6302 (2018)

192. M. Wen, J. Wang, R. Tong, D. Liu, H. Huang, Y. Yu, Z. K. Zhou, P. K. Chu, and X. F. Yu, A low-cost metal-free photocatalyst based on black phosphorus, *Adv. Sci. (Weinh.)* 6(1), 1801321 (2019)

193. T. Xue, W. Liang, Y. Li, Y. Sun, Y. Xiang, Y. Zhang, Z. Dai, Y. Duo, L. Wu, K. Qi, B. N. Shivananju, L. Zhang, X. Cui, H. Zhang, and Q. Bao, Ultrasensitive detection of miRNA with an antimonene-based surface plasmon resonance sensor, *Nat. Commun.* 10(1), 28 (2019)

194. R. Quhe, X. Peng, Y. Pan, M. Ye, Y. Wang, H. Zhang, S. Feng, Q. Zhang, J. Shi, J. Yang, D. Yu, M. Lei, and J. Lu, Can a black phosphorus Schottky barrier transistor be good enough? *ACS Appl. Mater. Interfaces* 9(4), 3959 (2017)

195. W. Zhou, J. Chen, P. Bai, S. Guo, S. Zhang, X. Song, L. Tao, and H. Zeng, Two-dimensional pnictogen for field-effect transistors, *Research (Wash. D. C.)* 2019, 1046329 (2019)

196. Y. Wang, M. He, S. Ma, C. Yang, M. Yu, G. Yin, and P. Zuo, Low-temperature solution synthesis of black phosphorus from red phosphorus: Crystallization mechanism and lithium ion battery applications, *J. Phys. Chem. Lett.* 11(7), 2708 (2020)

197. L. Kou, C. Chen, and S. C. Smith, Phosphorene: Fabrication, properties, and applications, *J. Phys. Chem. Lett.* 6(14), 2794 (2015)

198. M. R. Benzigar, V. D. B. C. Dasireddy, X. Guan, T. Wu, and G. Liu, Advances on emerging materials for flexible supercapacitors: Current trends and beyond, *Adv. Funct. Mater.* 30(40), 2002993 (2020)

199. J. Zhu, G. Xiao, and X. Zuo, Two-dimensional black phosphorus: An emerging anode material for lithium-ion batteries, *Nano-Micro Lett.* 12(1), 120 (2020)

200. T. Zhou, W. Pang, C. Zhang, J. Yang, Z. Chen, H. Liu, and Z. Guo, Enhanced sodium-ion battery performance by structural phase transition from two-dimensional hexagonal-SnS2 to orthorhombic-SnS, *ACS Nano* 8(8), 8323 (2014)

201. J. Choi, N. R. Kim, K. Lim, K. Ku, H. J. Yoon, J. G. Kang, K. Kang, P. V. Braun, H. J. Jin, and Y. S. Yun, Tin sulfide-based nanohybrid for high-performance anode of sodium-ion batteries, *Small* 13(30), 1700767 (2017)

202. X. Mei, T. Hu, Y. Wang, X. Weng, R. Liang, and M. Wei, Recent advancements in two-dimensional nanomaterials for drug delivery, *Wiley Interdiscip. Rev. Nanomed. Nanobiotechnol.* 12(2), e1596 (2020)

203. M. Qiu, A. Singh, D. Wang, J. Qu, M. Swihart, H. Zhang, and P. N. Prasad, Biocompatible and biodegradable inorganic nanostructures for nanomedicine: Silicon and black phosphorus, *Nano Today* 25, 135 (2019)

204. L. Cheng, X. Wang, F. Gong, T. Liu, and Z. Liu, 2D nanomaterials for cancer theranostic applications, *Adv. Mater.* 32(13), 1902333 (2020)

205. N. M. Latiff, W. Z. Teo, Z. Sofer, A. C. Fisher, and M. Pumera, The cytotoxicity of layered black phosphorus, *Chemistry* 21(40), 13991 (2015)

206. A. Naskar, S. Kim, and K. Kim, A nontoxic biocompatible nanocomposite comprising black phosphorus with Au–γ-Fe_2O_3 nanoparticles, *RSC Advances* 10(27), 16162 (2020)

207. T. Fan, Y. Zhou, M. Qiu, and H. Zhang, Black phosphorus: A novel nanoplatform with potential in the field of bio-photonic nanomedicine, *J. Innov. Opt. Health Sci.* 11(06), 1830003 (2018)

208. M. Zhu, Y. Osakada, S. Kim, M. Fujitsuka, and T. Majima, Black phosphorus: A promising two dimensional visible and near-infrared-activated photocatalyst for hydrogen evolution, *Appl. Catal. B* 217, 285 (2017)

209. Y. Zheng, Y. Chen, B. Gao, B. Lin, and X. Wang, Black phosphorus and carbon nitride hybrid photocatalysts for photoredox reactions, *Adv. Funct. Mater.* 30(30), 2002021 (2020)

210. N. Li, Z. Z. Kong, X. Z. Chen, and Y. F. Yang, Research progress of novel two-dimensional materials in photocatalysis and electrocatalysis, *J. Inorg. Mater.* 35(7), 735 (2019)

211. A. Yang, D. Wang, X. Wang, D. Zhang, N. Koratkar, and M. Rong, Recent advances in phosphorene as a sensing material, *Nano Today* 20, 13 (2018)

212. R. N. Pedrosa, R. G. Amorim, and W. L. Scopel, Embedded carbon nanowire in black phosphorene and C-doping: The rule to control electronic properties, *Nanotechnology* 31(27), 275201 (2020)

213. S. Xiao, H. Wang, Y. Qin, X. Li, H. Xin, G. Wang, L. Hu, Y. Wang, Y. Li, W. Qi, and J. He, Nonlinear optical modulation of MoS_2/black phosphorus/MoS_2 at 1550 nm, *Physica B* 594, 412364 (2020)

214. R. Zhao, J. Li, B. Zhang, X. Li, X. Su, Y. Wang, F. Lou, H. Zhang, and J. He, Triwavelength synchronously mode-locked fiber laser based on few-layered black phosphorus, *Appl. Phys. Express* 9(9), 092701 (2016)

215. X. Jin, G. Hu, M. Zhang, T. Albrow-Owen, Z. Zheng, and T. Hasan, Environmentally stable black phosphorus saturable absorber for ultrafast laser, *Nanophotonics* 9(8), 2445 (2020)

216. T. Wang, X. Jin, J. Yang, J. Wu, Q. Yu, Z. Pan, X. Shi, Y. Xu, H. Wu, J. Wang, T. He, K. Zhang, and P. Zhou, Oxidation-resistant black phosphorus enable highly ambient-stable ultrafast pulse generation at a 2 μm Tm/Ho-doped fiber laser, *ACS Appl. Mater. Interfaces* 11(40), 36854 (2019)

217. J. Y. Lee, J. H. Shin, G.H. Lee, and C.H. Lee, Two-dimensional semiconductor optoelectronics based on van der Waals heterostructures, *Nanomaterials (Basel)* 6(11), 193 (2016)

218. B. Yan, G. Li, B. Shi, J. Liu, H. Nie, K. Yang, B. Zhang, and J. He, 2D tellurene/black phosphorus heterojunctions based broadband nonlinear saturable absorber, *Nanophotonics* 9(8), 2593 (2020)

219. F. Lou, B. Zhang, S. Sun, C. Hu, Z. Lin, J. Jiang, S. Zhang, X. Wang, B. Teng, and J. He, Black phosphorus mode-locked sub-100 fs bulk laser based on heterostructured Yb composite crystal, *Appl. Phys. Express* 11(1), 012601 (2018)

220. Q. Liu, X. Wang, J. Wang, and X. Huang, Spatially controlled two-dimensional heterostructures via solution-phase growth, *Acta Phys.-Chim. Sinica* 35(10), 1099 (2019)

221. H. Yuan and Z. Li, Interfacial properties of black phosphorus/transition metal carbide van der Waals heterostructures, *Front. Phys.* 13(3), 138103 (2018)

222. Y. Song, K. You, J. Zhao, D. Huang, Y. Chen, C. Xing, and H. Zhang, A nano-lateral heterojunction of selenium-coated tellurium for infrared-band soliton fiber lasers, *Nanoscale* 12(28), 25933 (2020)